NAVAL POSTGRADUATE SCHOOL
Monterey, California

THESIS

STRUCTURAL CHARACTERISTICS OF DEAN
VORTICES
IN
A CURVED CHANNEL

by

Randal D. Niver

June 1987

Thesis Advisor Phillip M. Ligrani

Approved for public release; distribution is unlimited.

REPORT DOCUMENTATION PAGE

a REPORT SECURITY CLASSIFICATION UNCLASSIFIED	1b RESTRICTIVE MARKINGS
2a SECURITY CLASSIFICATION AUTHORITY	3 DISTRIBUTION/AVAILABILITY OF REPORT Approved for public release; distribution is unlimited
b DECLASSIFICATION/DOWNGRADING SCHEDULE	
4 PERFORMING ORGANIZATION REPORT NUMBER(S)	5 MONITORING ORGANIZATION REPORT NUMBER(S)
6a NAME OF PERFORMING ORGANIZATION Naval Postgraduate School	6b OFFICE SYMBOL (If applicable) Code 69
7a NAME OF MONITORING ORGANIZATION Naval Postgraduate School	
c ADDRESS (City, State, and ZIP Code) Monterey, California 93943-5000	7b ADDRESS (City, State, and ZIP Code) Monterey, California 93943-5000
8a NAME OF FUNDING/SPONSORING ORGANIZATION Propulsion Directorate	8b OFFICE SYMBOL (If applicable)
9 PROCUREMENT INSTRUMENT IDENTIFICATION NUMBER MIPR No. C-80019-F	
c ADDRESS (City, State, and ZIP Code) U.S. Army Aviation Res & Tech Activity AVSCOM NASA-Lewis Res. Center, Cleveland 45433	10 SOURCE OF FUNDING NUMBERS PROGRAM ELEMENT NO / PROJECT NO / TASK NO / WORK UNIT ACCESSION NO

11 TITLE (Include Security Classification)
STRUCTURAL CHARACTERISTICS OF DEAN VORTICES IN A CURVED CHANNEL

12 PERSONAL AUTHOR(S)
Randal D. Niver

13a TYPE OF REPORT	13b TIME COVERED	14 DATE OF REPORT (Year, Month, Day)	15 PAGE COUNT
Master's Thesis	FROM _____ TO _____	1987 June	63

16 SUPPLEMENTARY NOTATION

17 COSATI CODES			18 SUBJECT TERMS (Continue on reverse if necessary and identify by block number)
FIELD	GROUP	SUB-GROUP	Dean Vortices, Dean Number, Rectangular Curved Channel

Dean vortices in a curved channel were studied using flow visualization and a miniature Kiel probe to record total pressure. The channel is 1.27 cm. high by 50.8 cm. wide (0.5 in. x 20.0 in.), aspect ratio of 40 to 1, with a radius of curvature of 60.96 cm. (24.0 in.) for the concave surface. Mean velocities within the curve channel were maintained at Dean numbers which ranged from 0 to 250.

Smoke injected into the mouth of the channel at Dean numbers from 42 to 218 and locations from 65° to 145° revealed different types of flow behavior, including numerous pairs of Dean vortices extending from the convex to the concave wall. Different types of flow structures have been categorized as to unsteadiness, height, and symmetry. For each category a map has been constructed which depicts the flow structure

20 DISTRIBUTION/AVAILABILITY OF ABSTRACT ☒ UNCLASSIFIED/UNLIMITED ☐ SAME AS RPT ☐ DTIC USERS	21 ABSTRACT SECURITY CLASSIFICATION UNCLASSIFIED
22a NAME OF RESPONSIBLE INDIVIDUAL Phillip M. Ligrani	22b TELEPHONE (Include Area Code) (408) 646-3382 / 22c OFFICE SYMBOL 69Li

DD FORM 1473, 84 MAR 83 APR edition may be used until exhausted
All other editions are obsolete
SECURITY CLASSIFICATION OF THIS PAGE

Cont. Block 19

observed as a function of Dean number and angular location. These maps and the photographs give an understanding of the flow behavior in the curved channel over a significant range of experimental conditions.

Total pressure measurements at a Dean number of 110 and one location (118°) were taken. The preliminary results are presented on a contour plot which shows some repeatability across a 2 in. portion of the channel span. These contour plot results are consistent with photographs for the same experimental conditions.

Approved for public release; distribution is unlimited.

Structural Characteristics of Dean Vortices in a Curved Channel

by

Randal D. Niver
Lieutenant, United States Navy
B.S., Arizona State University, 1978

Submitted in partial fulfillment of the
requirements for the degree of

MASTER OF SCIENCE IN MECHANICAL ENGINEERING

from the

NAVAL POSTGRADUATE SCHOOL
June 1987

ABSTRACT

Dean vortices in a curved channel were studied using flow visualization and a miniature Kiel probe to record total pressure. The channel is 1.27 cm. high by 50.8 cm. wide (0.5 in. x 20.0 in.), aspect ratio of 40 to 1, with a radius of curvature of 60.96 cm. (24.0 in.) for the concave surface. Mean velocities within the curve channel were maintained at Dean numbers which ranged from 0 to 250.

Smoke injected into the mouth of the channel at Dean numbers from 42 to 218 and locations from 65^{o} to 145^{o} revealed different types of flow behavior, including numerous pairs of Dean vortices extending from the convex to the concave wall. Different types of flow structures have been categorized as to unsteadiness, height, and symmetry. For each category a map has been constructed which depicts the flow structure observed as a function of Dean number and angular location. These maps and the photographs give an understanding of the flow behavior in the curved channel over a significant range of experimental conditions.

Total pressure measurements at a Dean number of 110 and one location (118^{o}) were taken. The preliminary results are presented on a contour plot which shows some repeatability across a 2 in. portion of the channel span. These contour plot results are consistent with photographs for the same experimental conditions.

TABLE OF CONTENTS

LIST OF FIGURES

I. INTRODUCTION

A. BACKGROUND

Fully developed laminar flow near a concave wall does not maintain a simple two-dimensional velocity profile. On the contrary, many pairs of counter-rotating vortices form as a consequence of a centrifugal instability. The flow in a rectangular channel which is curved in the streamwise direction is an ideal environment for studying this type of secondary flow. Figure 1.1 [Ref. 1] is a schematic of how this secondary flow would appear in a curved channel.

W.R. Dean [Ref. 2] determined that the formation and development of vortices resulting from a centrifugal instability are dependent upon the magnitude of the wall curvature. He also found that this secondary flow would only be present if the dimensionless parameter $(Ud/\nu)\sqrt{d/R_i}$ were greater than 36.6. This quantity is now defined as the Dean number where, U is the mean streamwise velocity, d is the channel height, R_i is the radius of curvature of the convex wall, and ν is the kinematic viscosity.

Dean Vortices form in curved channels as a result of the fluid particles in the center of the flow profile which travel at higher velocities than particles near the wall. The higher velocity fluid particles are subjected to greater centrifugal forces which direct them outward toward the concave wall. As a result of this action, particles already at the concave wall are forced to move inward toward the center of the channel where the velocities are higher. This process is repeated again and again throughout the curved channel, resulting in pairs of counterrotating vortices, often referred to as Dean vortices. Numerical simulations of the Navier-Stokes equations for similar vortex structures have been made by Finlay, Keller, and Ferziger [Ref. 3]. The present experiment was undertaken partially to validate their findings. In addition, the effect of secondary flows on transition, especially the onset, and on heat transfer, are the ultimate goals of the overall project of which this thesis is a part.

Other recent work has been undertaken by Kelleher, Flente, and McKee [Ref. 4] who studied secondary flows in a curved channel half the size of the facility used in the current study.

Other relevant studies in the open literature include ones by Nakabayashi [Ref. 5], Williams, Fasel, and Hama [Ref. 6], Nishioka and Asai [Ref. 7], Hille, Vehrenkamp, and Schulz-Dubois [Ref. 8], and Georgiou and Eagles [Ref. 9]. Of these, Nakabayashi [Ref. 5] used flow visualization to observe fourteen different regimes in flow between two concentric rotating spheres with the inner one rotating and the outer one stationary. Included in the observations were several different types of toroidal Taylor-Gortler vortices. Williams, Fasel, and Hama [Ref. 6] studied the three-dimensional vorticity field during lanimar-turbulent transition. Highly inflexional shear layers were observed which break down into hairpin vortices. Nishioka and Asai [Ref. 7] introduce cylinder-generated vortical disturbances into plane Poiseulle flow to show that the minimum transition Reynolds number is about 1000 and related to the external disturbance triggering transition. Hille, Vehrenkamp, and Schulz-Dubois [Ref. 8] studied the development and structure of primary and secondary flow in a curved square duct. Georgiou and Eagles [Ref. 9] used analysis to examine the stability of flows in channels with small wall curvature.

Flow visualization provides an excellent means of obtaining an overview of flow behavior. Some flow details may also be discerned, however, it may be used most advantageously to determine when certain types of flow behavior are present and when they are not. In this study, of special interest are locations and Dean numbers where pairs of counterrotatng vortices form, and then,where these vortices begin to oscillate, and become unstable resulting in the formation of turbulent spots. A beginning was provided by Siedband's study [Ref. 10] however, his results were obtained only by using a smoke wire. In the present experiments, streams of smoke are introduced into the channel giving observers more informative pictures as to what events are occuring, where they are taking place, how various flow structures develop with downstream distance, and how such structures are altered with Dean number.

B. OBJECTIVES

The objectives are:

1. Modify the existing curved channel so that Dean numbers between 0 and 250 may be obtained using a new blower.
2. Provide extensive photographic evidence of the flow behavior in the curved channel as a function of the radial location and Dean number.
3. Obtain preliminary quantitative measurements of total pressure distribution across a number of vortex pairs.

II. EXPERIMENTAL FACILITIES

A. CURVED CHANNEL

The curved channel used in the present study is described by Siedband [Ref. 10] A schematic is shown in Figure 2.1. Figures 2.2 and 2.3 show photographs of front and side views.

B. BLOWER #2

An additional blower was added to the channel in order to achieve lower flow rates than employed by Siedband. The suction side of this blower is connected to a plenum (labelled #2 in Figure 2.1). This plenum is connected to a 2 in. line leading to another valve (labeled 1). From valve 1, 2 in. piping leads to an orifice plate and finally to plenum # 1. Plenum # 1 is larger than # 2. The purpose of plenum # 1 is to provide a box of uniform, low pressure air at the exit of the channel. Plenum # 2 was used as a means to mate the 5.5 in. diameter blower inlet to 2 in. piping without significant pressure losses in the system. The throttle valve is a brass globe valve while the bypass valve is a PVC ball valve. The orifice plate is a 1.5 inch, ASME type and the pipe connecting all of the components is standard 2 inch PVC pipe. Occasionally, a 1.0 in. ASME orifice plate ia also used, but only for very low flow rates.

The newly added blower #2 is a type 10P manufactured by ICG industries. Blower # 1 produces 60 inches of water vacuum at 140 CFM ; whereas, blower # 2 is rated for 4 inches of water vacuum at 170 CFM. Each system is completely isolated from the other, when one or the other is used to operate the channel. Figure 2.4 shows blower #2 performance data from the manufacturer, and a curve showing channel pressure change versus flow rate without an orifice plate.

C. THE SMOKE GENERATOR

Smoke was injected into the channel to provide visualizations of flow behavior. The smoke generator was first designed and used by Morrison [Ref. 11]. Figure 2.5 shows a schematic. In the generator, smoke is initially produced by burning mesquite wood chips in a 3 inch diameter, 16 inch long vertical steel pipe. Mesquite was chosen since it resulted in dense, white smoke, easily visible against the black paper used to line the outside of the channel convex surface. Once the pipe is filled with wood chips,

the upper opening is sealed by a flange. The flange houses the wire mesh screens used for filtering. Connected to the flange is tubing linking the pipe to a sealed glass jar. This jar is used to collect unwanted combustion particles and water vapor from the smoke fumes as they are removed in the cooling system located above. This cooling system consists of two coiled tubes enclosed by flowing water. The smoke is directed via a rubber hose to a smoke rake located at the inlet to the channel. This rake consists of a small plenum chamber with 9 pipes used to direct the flow.

Combustion is initiated by energizing a nichrome wire heating coil at the bottom of the column of wood chips. Compressed air is provided at a pressure of 4-8 psig to the base of the steel pipe near the heating coil for combustion and to force the smoke through the system.

The smoke generated by the apparatus was dense, cool and in sufficient quantity to permit detailed observations of the flow structures under study. The system had a number of drawbacks, since it could produce smoke only for a short amount of time (5 to 10 min.) before requiring refueling. Refueling before the system had cooled down was difficult and hazardous due to the high temperatures in the vicinity of the steel pipe. A thick, tar-like residue was always present at the tips of the smoke rake during generation of smoke. This residue did not collect on the interior walls of the channel, however it did produce a film on the inside of one of the rotameters.

D. LIGHTING/CAMERA

The flow visualization techniques used in this study required two different lighting systems. (1) The first was used for visual observations only, and consisted of a General Radio Type 1531-A Strobotac set at a strobe rate of 2400 flashes per minute. It was necessary to focus the light using a columnator lens because of the strobes long distance (15 inches) from the point of interest. (2) The second was employed when smoke patterns were photographed. Here a Nikon SB-16 speedlight provided the necessary lighting. The camera and flash are synchronized by means of a through the lens metering system. This system allows the camera to measure the amount of light entering the camera from the flash unit and automatically determine the proper shutter speed for the best exposure.

A Nikon F-3 camera body with a 55mm, f-2.8 lens was used to record flow patterns on film. The camera was mounted on a tripod for stability and to maintain the proper focus. Figure 2.6 shows the relative locations of the camera, strobe, lens and channel. An aperture setting of f4.0, shutter speed set for automatic (A), and

speedlight adjusted for TTL produced the best pictures with the smoke generator. The film which produced the highest resolution photographic prints was Kodack Tri-X (ASA 400).

The outside of the convex surface of the channel is covered by black poster board to prevent undesired light reflecting or leaking into the photographic region. Slits 0.2 cm x 4.6 cm (0.079 in. x 1.8 in), centered 5 cm (2.0 in.) off of the channel centerline were cut into the poster board. These slits provided a means to locate paths of light at locations spaced at 5 degree intervals from 0 to 185 degrees around the circumference of the channel.

E. CHANNEL TRAVERSING/DATA ACQUISITION SYSTEM

Total pressure measurements in the channel were made using a miniature Kiel probe, Celesco pressure transducers and demodulators, a Hewlett-Packard 3497 data sampler, a Hewlett-Packard 9836S microprocessor, and a MITAS Two-Axis motion controller driving the traversing mechanism.

The Kiel probe is a type KAA-8, manufactured by United Sensor, with a .066 in. outer diameter shield around the probe. This was chosen to provide a minimal amount of flow blockage in the channel. An automated traversing mechanism was used for probe positioning. The probe is mounted on a vertically mounted traversing carriage, which in turn is mounted on a block which moves in the spanwise direction. Each traversing block is moved using a 20-thread per inch drive screw and two ground steel, case-hardened steel guide/support shafts. Each drive shaft is directly coupled to a SLO-SYN type MO92-FD310 stepping motor. The motors are controlled by a MITAS Two-Axis Motion Controller, Figure 2.7. The stepping motors and the controller are manufactured by Superior Electric Company. The controller directs the movement of the probe in the spanwise and vertical directions. The MITAS controller comes equipped with 2K bytes of memory and an MC68000, 16-bit microprocessor which allows the user to control the start, stop, duration, speed, acceleration and deceleration of each step made by the motors.

The probe is connected through plastic tubing to a Celesco model LCVR differential pressure transducer. The transducer has a designed pressure range of 0 - 2 cm (0 - .75 in.) water and produces a 25 mV/volt output signal. The transducer output signal is converted to a proportional DC signal by Celesco CD10D carrier demodulators. Each demodulator has a maximum frequency response of -3dB at 500 Hz and a maximum output noise of 10mV, peak to peak. Each transducer/carrier

demodulator combination was calibrated against a Meridian 1.27 cm (.5 in.) horizontal manometer with an accuracy of 0.002 cm (0.005 in.) of water. Typically, the system for measuring pressure produced 1 volt for 0.1 in. of water differential pressure.

The computer and data acquisition system shown in Figure 2.8 acquires the voltages from each pressure transducer and converts each voltage to a pressure. The computer is a Hewlett-Packard 98365S. Configured with 1M byte of memory and a single magnetic tape cartridge drive, the HP-9836S was used to collect, store, display, and print the majority of the data required. The transducer/carrier demodulator is connected directly to the HP-3497 data acquisition/control unti. The HP-3497, which provides precision measurement and process monitoring, is equiped with analog multiplexing and a digital voltmeter with 1 μ V sensitivity. A HP 7470 two pen plotter was used for graphic representation of the data.

Two software programs were developed for use during the thesis. TPACQ3 was used to record, time-average, and store the pressure measurements. PLOT3 was developed to plot the results. The programs are a simplification of those created by Evans [Ref. 12]. Through the Basic program TPACQ3 the user is prompted for the number of spanwise and vertical data points and resolution. This is followed by the prompt to manually calibrate each transducer against a horizontal manometer. The final step requires that the traversing mechanism and the DAS be initiated simultaneously. Data taking from this point on is totally automated.

III. EXPERIMENTAL PROCEDURES

A. CHANNEL OPERATION

A new blower was connected to the channel in order to achieve lower flow rates than available with the blower used by Siedband [Ref. 10]. The suction side of the blower was connected so that the channel plenum was below atmospheric pressure. The operation of the second blower (hereafter, denoted blower #2) was quite simple. Any flow rate (and Dean number) could be easily set and repeated by referring to the pressure drop across an orifice plate, located just upstream of plenum #2 (shown in Figure 2.1). Flow rate changes were made by throttling a gate valve between plenum #1 and plenum #2, while a bypass valve to plenum #2 was kept open.

The blower is started with all valves connected to blower #1 closed (A, B, & C of Figure 2.1) and the 1 in. bypass valve on plenum #2 open. Unlike blower #1 which has a strong tendency towards unsteadiness at very low Dean numbers, blower #2 produced no noticable flow oscillations.

In order to further understand the channel behavior, several simple qualification tests were conducted. Because of the flow manegment devices used at the inlet of the channel, most of any flow blockage just at or in front of the inlet had no discernable effect, even if one-third of the inlet is covered. However, unsteady disturbances at the inlet had more noticable effect. Consequently, it was attempted to conduct tests, whenever possible, without disturbances in or near the laboratory due to passage of people, opening doors, etc.

B. FLOW RATE MEASUREMENTS

Flow rate measurements were achieved using a 1.5 in. diameter steel orifice plate, machined to ASME specifications, installed upstream of the throttling valve in the 2 in. inner diameter pipe. Orifice tapes were located at 1-D (2 in.) upstream and .5-D (1 in.) downstream of the orifice plate. The pressure tapes were connected to a Meridian manometer with a 0.0 to 0.5 in. pressure range. Appendix B provides the sample calculations for mass flow rate and the conversion to Reynolds number and Dean number. Ambient air pressure and temperature were recorded at each flow rate measurement condition.

A series of comparison tests between blower #1 and blower #2 were performed to verify the flow rate calculations for the channel. The test procedure required recording pressure drops at plenum #1 with respect to atmospheric pressure, as the magnitude of channel flow is a result of this pressure drop. Simultaneously, the pressure drop across the orifice plate for the blower under test is likewise recorded. Flow was controlled by adjusting the blower's throttling valve (valve A for blower #1 and valve 1 for blower #2). Results of these tests are given in Figure 3.1. Here $P_{atm} - P_{plenum}$ is shown as dependent upon flow rate in CFM. Also included on Figure 3.1 are results of a test with a 1 in. diameter orifice plate installed upstream of blower #2. The results for each system agree, providing a cross-check of flow rate measurements. For the calculations, ASME tables of flow coefficients (see Appendix B) were employed. For the 1.5 in. orifice plate, these were in agreement with an updated empirical ASME formula within 3 percent.

Pressure drop across the orifice plate and pressure drop from channel inlet to the upstream side of the orifice plate provided the necessary data to calculate the Dean number during experiments. The Dean number is a linear function of mass flow rate as seen in Figure 3.2. Figure 3.3 was used during flow visualization and total pressure tests to determine Dean number directly from pressure drop across the orifice plate.

C. FLOW VISUALIZATION/PHOTOGRAPHY

Once the channel was operating at the desired Dean number, the smoke produced in the smoke generator was injected into the mouth of the channel (Figure 3.4). Observations were easily made at 5^{o} intervals around the channel's radius using a strobe light source rotated such that light was directed to different angular positions. Using this method, the evolution of the smoke patterns could be followed around the channel for each selected flow rate. Alternatively, it was also possible to keep the strobe at one location and vary the flow rate; thereby, noting structural developments in the smoke patterns as a function of Dean number.

Photographs were taken by replacing the observer with the camera and substituting the camera flash unit for the strobe. The camera was set on a tripod at the desired spot and properly focused. Taking a photo then required holding the flash unit in one hand approximately 6 in. from the convex side of the channel, 90^{o} to the camera's line of sight and pressing the camera shutter. The photos were always taken so that the pictures look downstream. A series of 2-5 pictures were normally taken in rapid succession (1-2 seconds apart) at each Dean number at a given location. A

period of 30 to 40 seconds was required to insure that a steady state flow was present in the channel after a flow rate adjustment.

D. TOTAL PRESSURE MEASUREMENTS

The channel was modified to permit total pressure measurements. A slot 0.32 cm (1/8 in.) wide and 7.62 cm (3.0 in.) long was cut in the convex wall of the curved channel. It was aligned in the spanwise direction 5.08 cm (2.0 in.) off the centerline at the 118^{o} location. The slot was lined with foam to allow insertion of the miniature Kiel probe into the channel and still prevent air leakage. A great deal of care was taken to ensure no foam extended into the channel to disrupt the flow of the slot. A small step was present at the slot/foam location, which probably provided some flow disturbance just downstream, though no effect were expected nor seemed to be present just upstream or at the probe location. A support block of Lexan 15.24 cm x 7.62 cm x 2.54 cm (6.0 in. x 3.0 in. x 1.0 in.) was also glued to the wall surrounding the slot to maintain the convex wall's dimensions and structural integrity.

The traversing mechanism was mounted to the channel support frame (Figure 3.5) and angled so the probe was normal to the wall. The probe was positioned in the traversing mechanism so it's center was 0.127 cm (0.05 in.) from the concave wall. The pressure transducer is located within 3 in. of the end of the miniature Kiel probe to minimize the distance over which the small pressure variations must be detected. At present, the movement of the probe is not controlled by the data acquisitioning system (DAS), but by the MITAS processor. Consequently, timing of the DAS and the MITAS controller must be adjusted such that probe movement and data acquisition are synchronous. This is most easily accomplished by adjusting the delay time in MITAS used for controller software.

Three channels of the DAS were employed in the study. One was used for the total pressure from the Kiel probe. The second was used for the pressure measured at plenum #1. The third was for ambient temperature. Details of the hardware and software operation are presented in Chapter 2, section E.

As preliminary total pressure measurements were made, small leaks existed through the foam which were believed to significantly affect results. This foam was replaced with new foam, installed such that no apparent leaks existed, and more sensible data was obtained. Foreign matter such as bits of plastic, dirt, and oil droplets also seemed to have an effect on pressure readings, since a further improvement in readings resulted after the channel was cleaned. In addition, the best results were

obtained when measurements were made at times when the laboratory and surrounding area were totally desserted, providing additional evidence on the imprortance of minimizing unsteady inlet disturbances.

IV. RESULTS

A. FLOW VISUALIZATION

Flow features shown in photographs at different locations and Dean numbers are described in terms of four categories of fluid mechanics behavior. Each category describes a specific feature of the flow. The categories are: type of flow, unsteadiness, height, and symmetry. The photographs cover a distance of 1.8 in. in the spanwise direction and the full channel width of .5 in. The camera's flash illuminates a channel section in the radial plane normal to the flow direction. The flow is into the photograph with the concave wall at the bottom and the convex wall at the top.

A. Type of Flow--This category describes the overall qualitative description of the type of flow present at a given Dean number and at a specific angular location.

1. Smoke Layer--Smoke is present across all or a portion of the channel width without evidence of any sort of vortex motion (Figure 4.1).
2. Incomplete Vortices--Incomplete vortices are considered to be present when distorted smoke layers which have a generally wavy appearance near the concave side of the channel exist. In some cases, such flows appear to contain circular "vortex-like" structures which have not made complete rotations (Figure 4.2).
3. Dean Vortices--Evidence that pairs of counter-rotating Dean vortices are present is indicated by mushroom-shaped smoke patterns periodically spaced across the channel span. These "mushrooms" emerge from the concave wall and extend to the convex wall. In almost every case observed, about 3.5 vortex pairs seem to be present and at the same location regardless of the experimental condition. In some cases, some turbulence may be present in flows classified using this category (Figure 4.3).
4. Flow with Turbulence--In this category, so much turbulence is present that any type of vortex or swirling motion is nearly unidentifiable (Figure 4.4).

B. Unsteadiness--The level of unsteadiness is identified quantitatively from 2-5 sequential photographs at each experimental condition. These oscillations were observed in both the radial and spanwise directions.

1. Low Unsteadiness--The flow pattern remains almost totally unchanged with time. In some cases, a small amount of spanwise oscillation is discernable (Figure 4.5).

2. Moderate Unsteadiness--Dean vortices are easily recognizable; however, during oscillations the mushroom stems are no longer normal to the concave wall but are highly skewed toward the channel sidewalls as they oscillate (Figure 4.6).

3. High Unsteadiness--Dean vortices are identifiable but mushroom shapes are deformed and significantly contorted with time in both spanwise and radial directions, especially the former (Figure 4.7).

4. Super High Unsteadiness--The mushroom shapes of the Dean vortices are severly wrenched out of shape as time progresses, such that vortex shapes are nearly unidentifiable (Figure 4.8).

C. Height--At some measureable conditions, all or some of the mushroomedshaped smoke patterns occupied less than the full width of the channel

1. Full Height--The mushroom-shaped smoke patterns extend the complete channel width (Figure 4.9).

2. Partial Height--The mushroom-shaped smoked patterns are only a fraction of the full channel width and do not extend completely from the concave wall to the convex wall (Figure 4.10).

3. Mixed Height--Different mushroom-shaped smoke patterns have different heights at different spanwise locations (Figure 4.11).

D. Symmetry--In flows where evidence of vortices is present, the symmetry of the smoke patterns is considered by comparing smoke pattern shapes on opposites sides of radial lines of symmetry.

1. Axisymmetric--The vortex forms are nearly exact mirror images across the line of symmetry (Figure 4.12).

2. Non-Axisymmetric--The Dean vortex pair is distorted to such an extent that no line of symmetry exists (Figure 4.13).

Four maps were created to relate the Dean number/location to each of the categories described above. Maps showing type of flow, stability, symmetry, and height are given in Figures 4.14 through 4.17, respectively. Locations where photographic evidence is available is marked on each map by solid circles. Quality pictures at angular positions less than 65° or greater than 145° were not possible because of the of light reflected from the flash against the Lexan sidewalls at large and small angles. Though visual observations were made at channel locations ranging from 20° to 180°, Figures 4.14 - 4.17 are based solely on photographic results.

Two photographic surveys are presented to illustrate the development of the flow structure with (a) changing location and constant Dean number, and (b) constant location and changing Dean number. Figures 4.18 to 4.28 present a series of pictures at the 115° location where the Dean number varies from 41 to 218. These series of

photographs depict the flow structure changing from a smoke layer, to a region of incomplete vortices to Dean vortices. The steadiness is seen to vary from low unsteadiness at Dean numbers less than 90 to moderate unsteadiness, then to high unsteadiness at Dean numbers between 160 and 200, above which the flow turns to super-high unsteadiness. The flow becomes non-axisymmetric at a Dean number of about 115. The Dean vortices are seen to be of mixed height at Dean numbers between 70 and 95 and full height at Dean numbers greater than that. Of particular interest in this sequence of photographs are the rapid formation of mushroom patterns between Dean numbers of 64 and 73, and significant pattern distortions which occurs between Dean numbers of 163 and 192.

Figures 4.29 to 4.37 show the progression of the flow characteristics by changing the angular location from 65^{o} to 145^{o} with the Dean number constant at 122. The flow structures are seen to begin as incomplete vortices which remain until 85^{o} and then become fully-formed at the 95^{o} location. At this Dean number the flow show only low and moderate unsteadiness, changing at the 105^{o} position. The Dean vortices remain axisymmetric until 115^{o} and then become non-axisymmetric. The change from partial height to mixed height occurs at 95^{o} and then goes to full height around the 105^{o} location. In this sequence of photographs, particularly significant changes occur between the 125^{o} and 135^{o} locations, and between the 85^{o} and 95^{o} locations.

Also of interest are results from Finlay [Ref. 13] plotted on Figure 4.15 . This line represents his prediction as to where pairs of Dean vortices develop twisting waves for moderate amounts of pressure disturbances at the inlet. This line corresponds roughly with observations of the onset of asymmetric pairs of Dean vortices and moderate unsteadiness.

B. TOTAL PRESSURE

The total pressure field in one plane was measured using a miniature Kiel probe to measure total pressure. A miniature Kiel probe was used because of its small size, and because of its insensitivity to flow direction. Data were taken at 8 different vertical locations, each with 40 spanwise positions, to equal a total of 360 points. This is equivalent to 2.0 in. in the spanwise direction and .4 in. in the radial direction. The measurements were made at a Dean number of 110 and at the 118^{o} location around the channel.

The results are presented in Figure 4.38 as a contour plot. The abscissa represents distance in the Z-direction. The ordinate represents distance in the Y-

direction. The left Y-axis represents a location 2 in. off the centerline. The shapes of the contour lines show some repeatability across the plane of the measurements. At this location and Dean number, the photographs show that axisymmetric Dean vortices are present with moderate unsteadiness and full height.

V. CONCLUSIONS AND RECOMMENDATIONS

Some characteristics of flow in a curved channel with a 40:1 aspect ratio have been observed. Unsteadiness, height, symmetry, and the type of flow generated are the categories used to describe the most distinctive features. Separate flow regimes are present which are a function of both the Dean number and the angular position around the channel.

The appearance of Dean vortices was shown to vary greatly with Dean number and angular position from the start of the curve. At Dean numbers less than 90, vortices do not form until 90^{o} around the channel. At Dean numbers greater than 180, vortices form at 75^{o}. Prior to the formation of complete vortices, the change of the character of the flow is from smoke layer to incomplete vortices. This change of the character of the flow can be quite rapid at large angles. Figure 4.14 shows that for channel positions of less than 85^{o} the region where incomplete vortices form range from Dean numbers 70 to 160. At Channel locations greater than 105^{o} incomplete vortices are seen only at Dean numbers 50 to 70.

Pairs of Dean vortices become gradually more unsteady with increasing Dean number and increasing angular position. Similarly, increasing the Dean number, angular position or both will result in less symmetric vortex pairs. The transition from partial to mixed to full height, on the other hand, was more abrupt and occurred over a smaller range of angular positions.

The contour plot of total pressure indicated a spanwise repeatability of high and low pressure zones. In some cases, those zones also revealed a preferred orientation or direction. The results are very preliminary and require much further investigation. In particular, the relation between contours and observered smoke patterns must be understood. In addition, results from the present experiment need to be repeated, and undertaken over a wider range of Dean numbers.

APPENDIX A
FIGURES

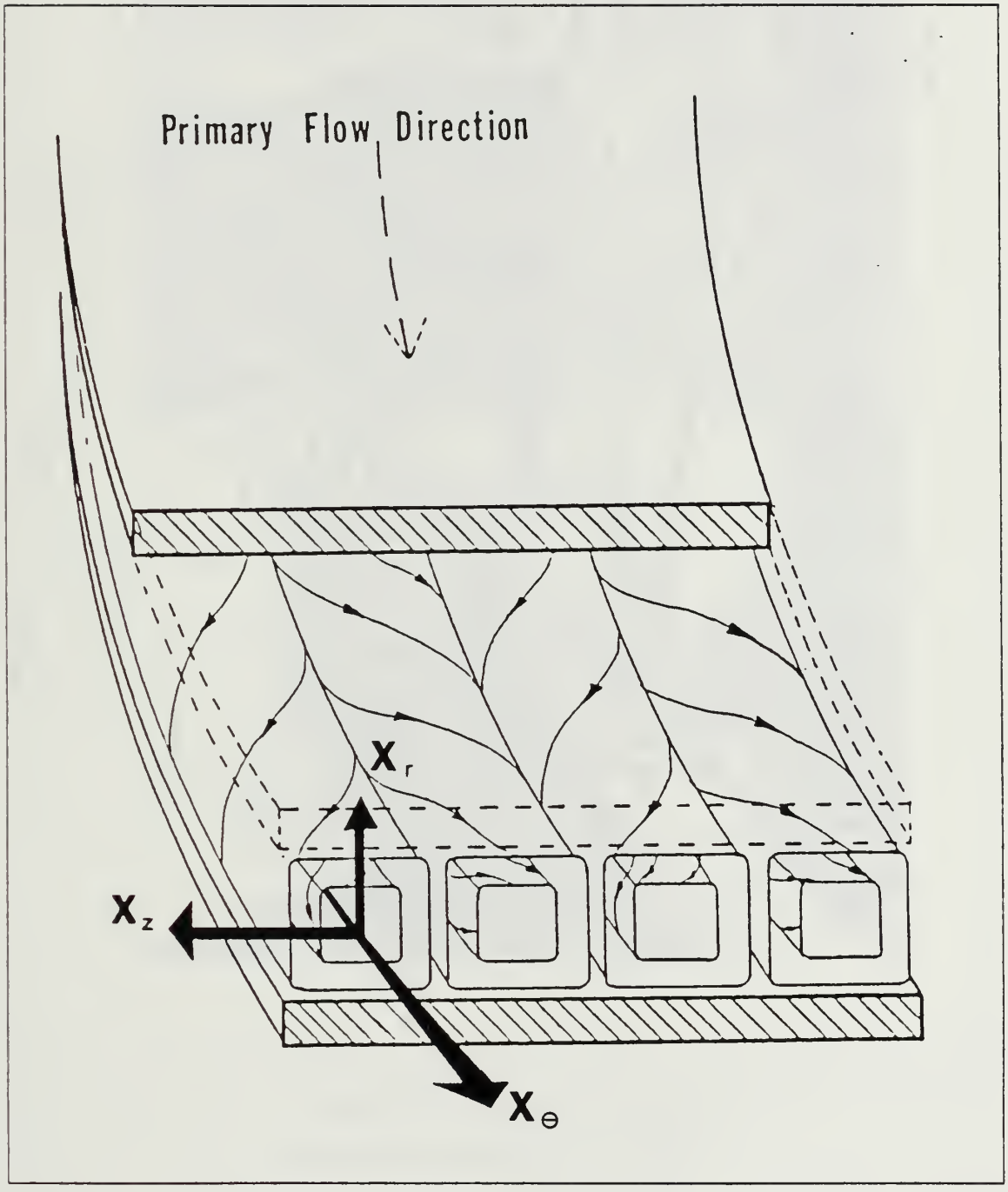

Figure 1.1 Schematic of Dean vortices in a curved channel.

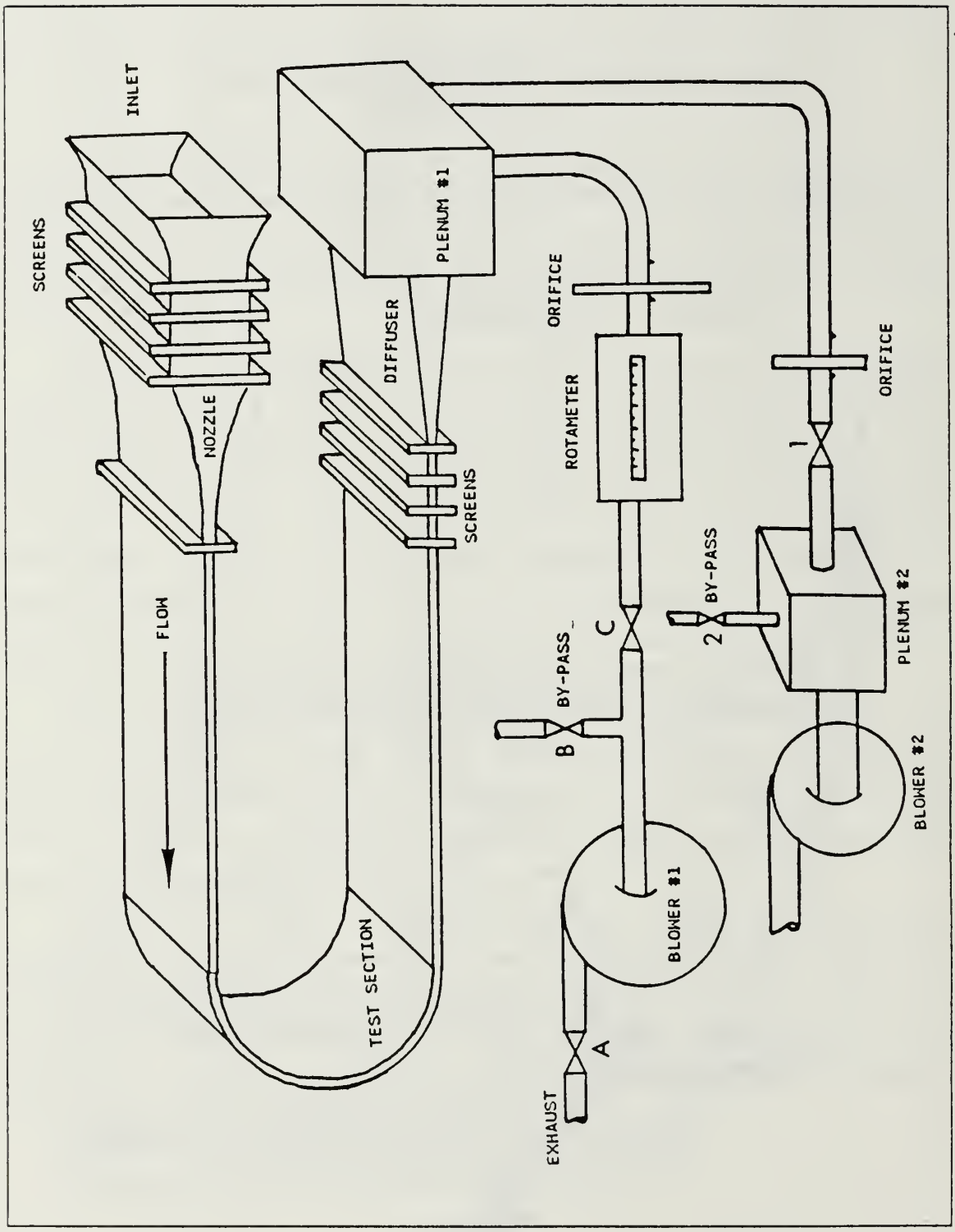

Figure 2.1 Schematic of test facility.

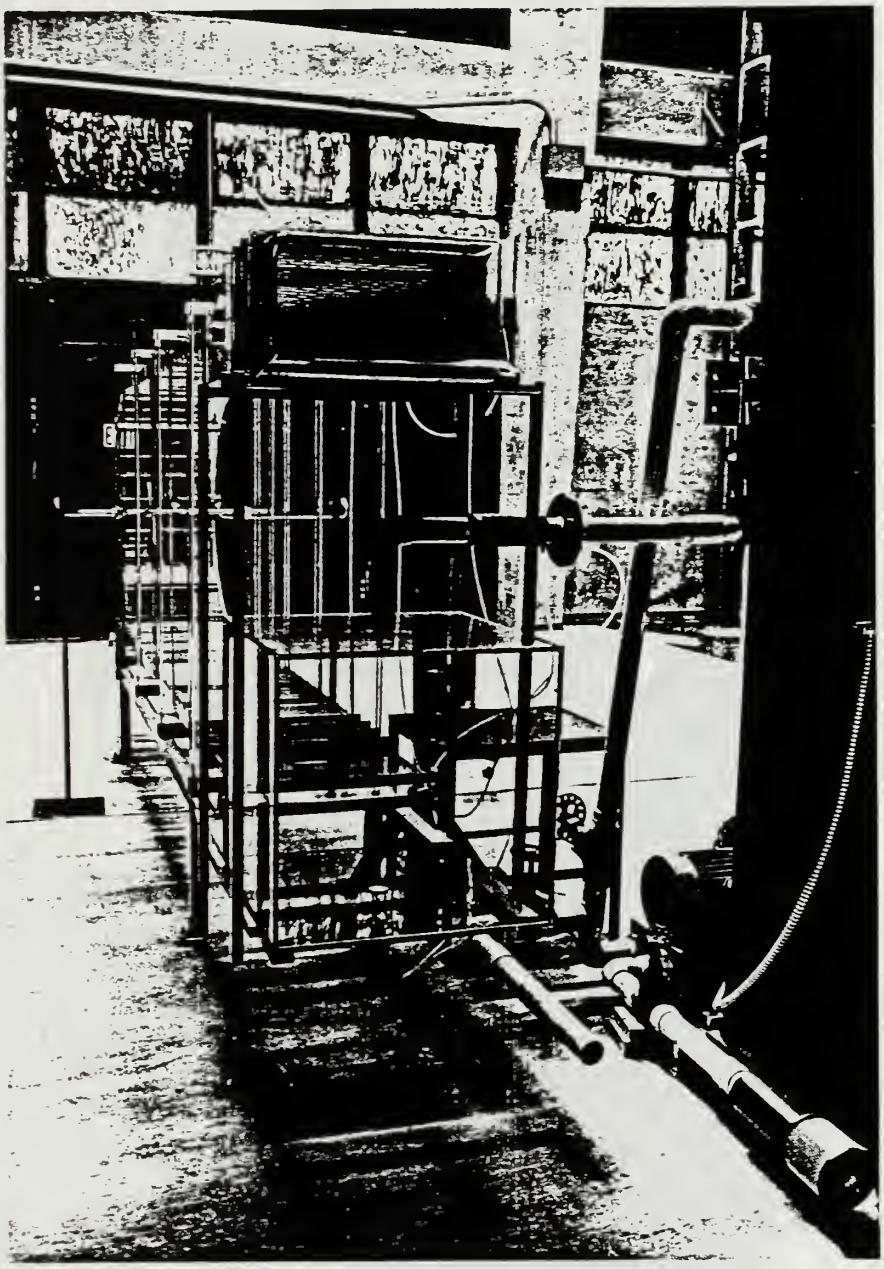

Figure 2.2 Test facility (front view).

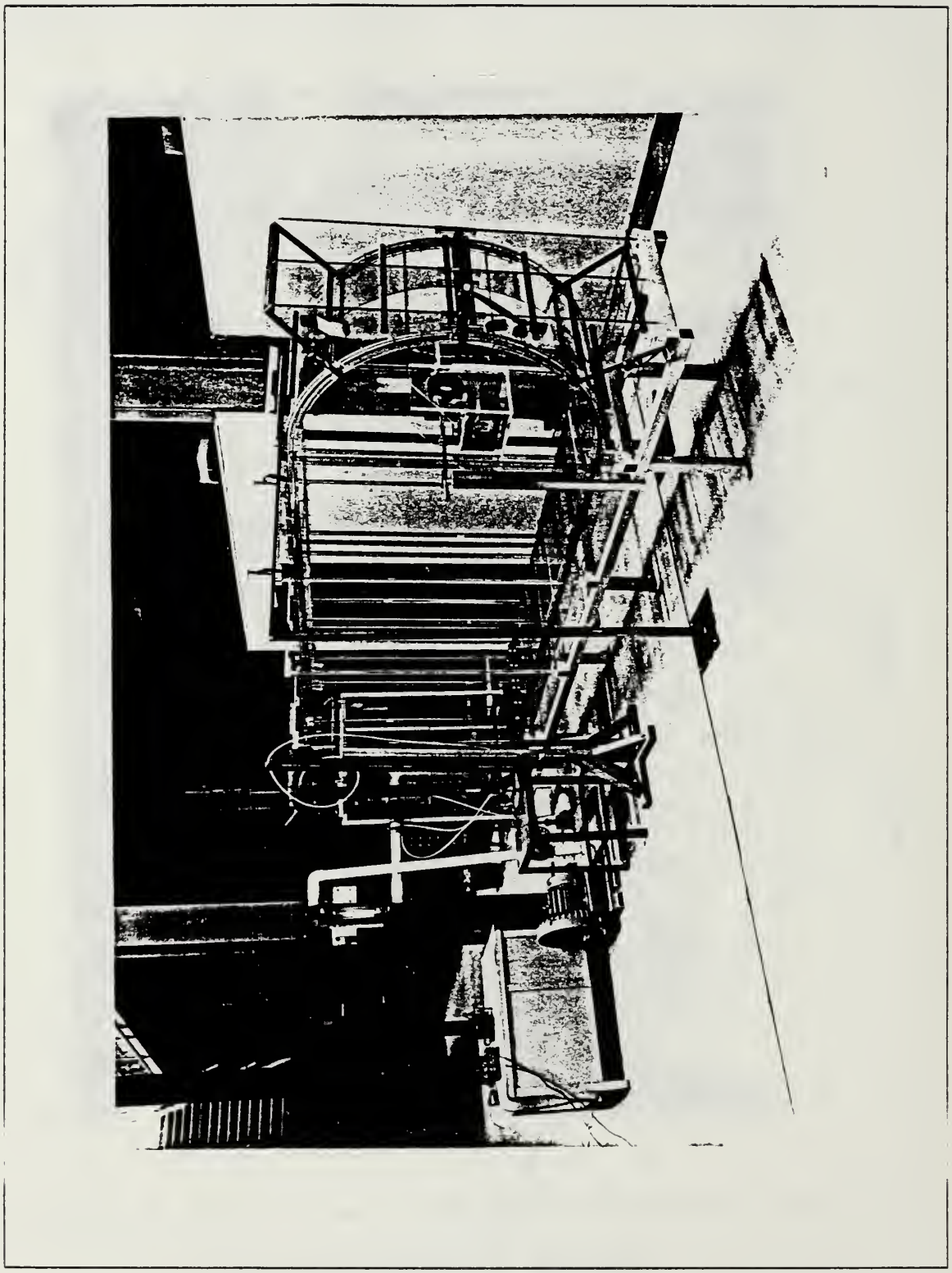

Figure 2.3 Test facility (side view).

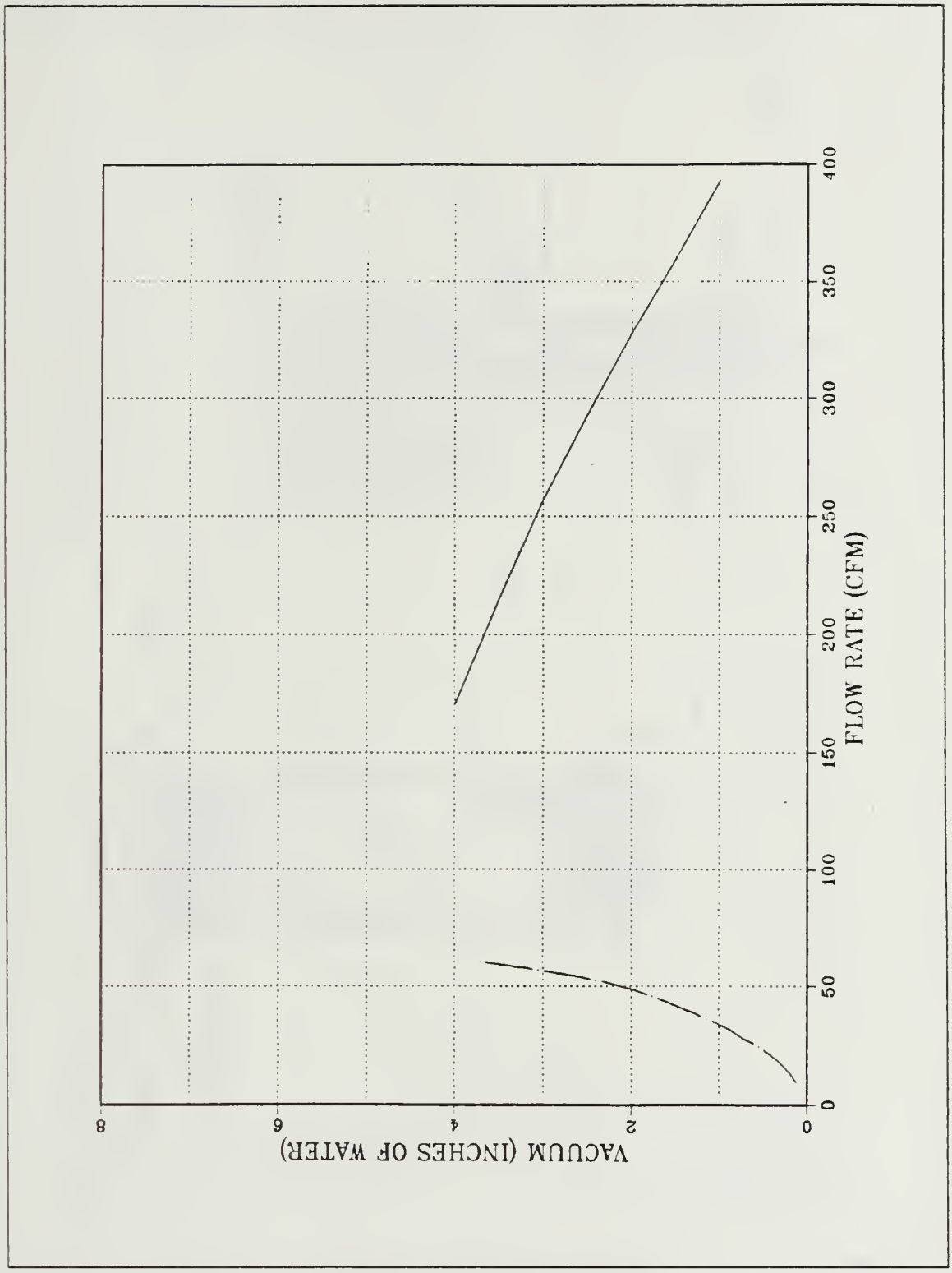

Figure 2.4 Blower Performance and System Curves.

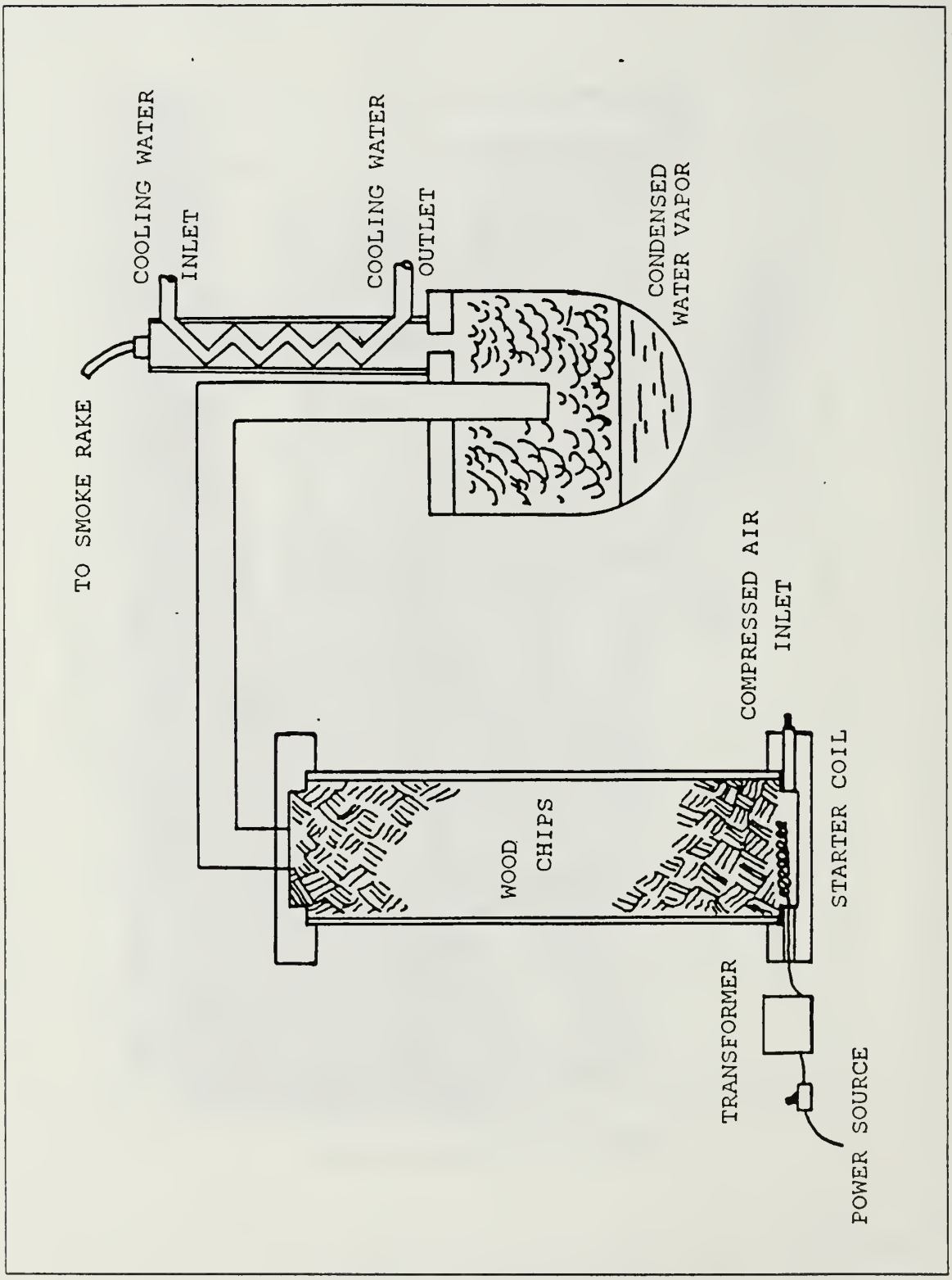

Figure 2.5 Schematic of the smoke generator.

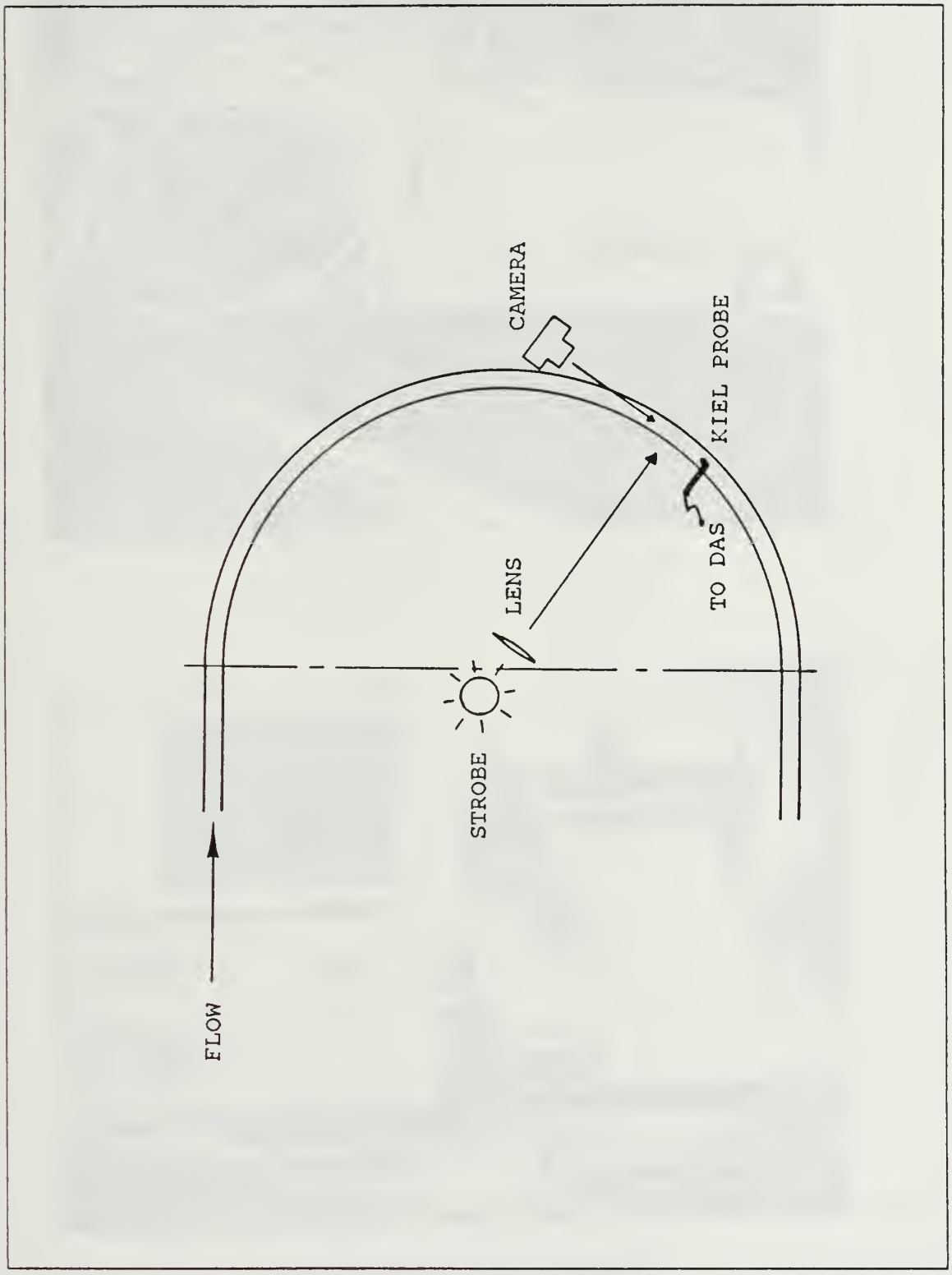

Figure 2.6 Schematic of strobe, camera, and total static pressure probe location.

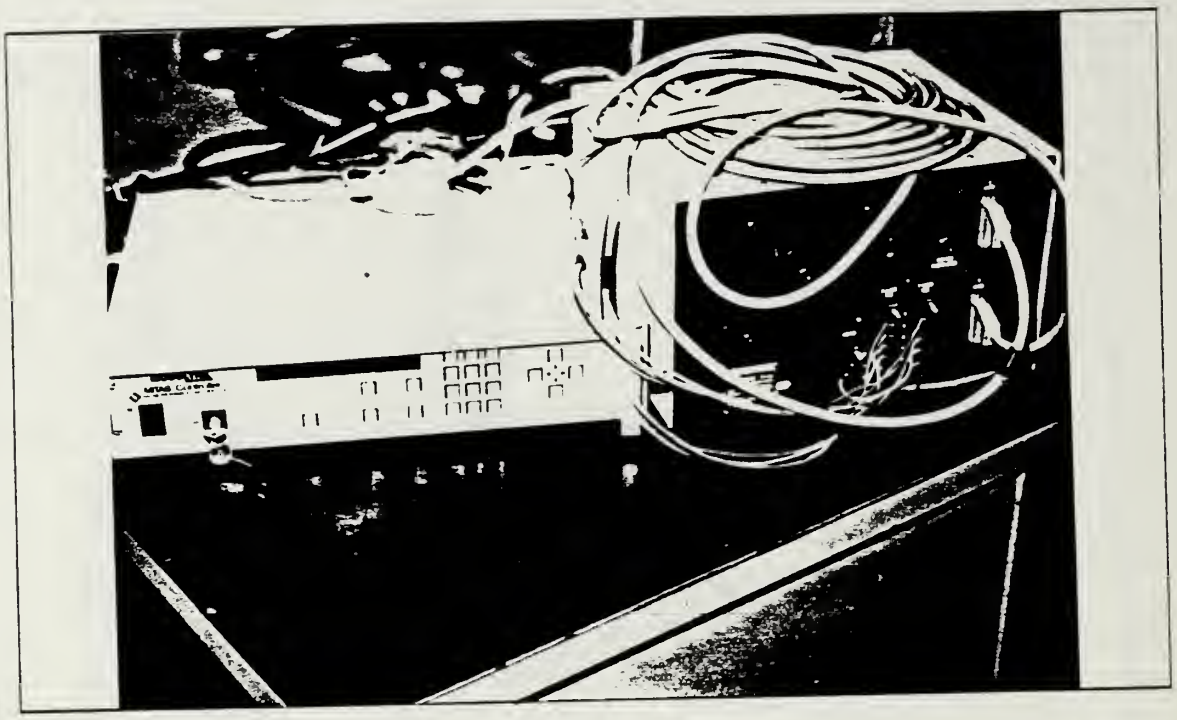

Figure 2.7 Two-axis motion controller.

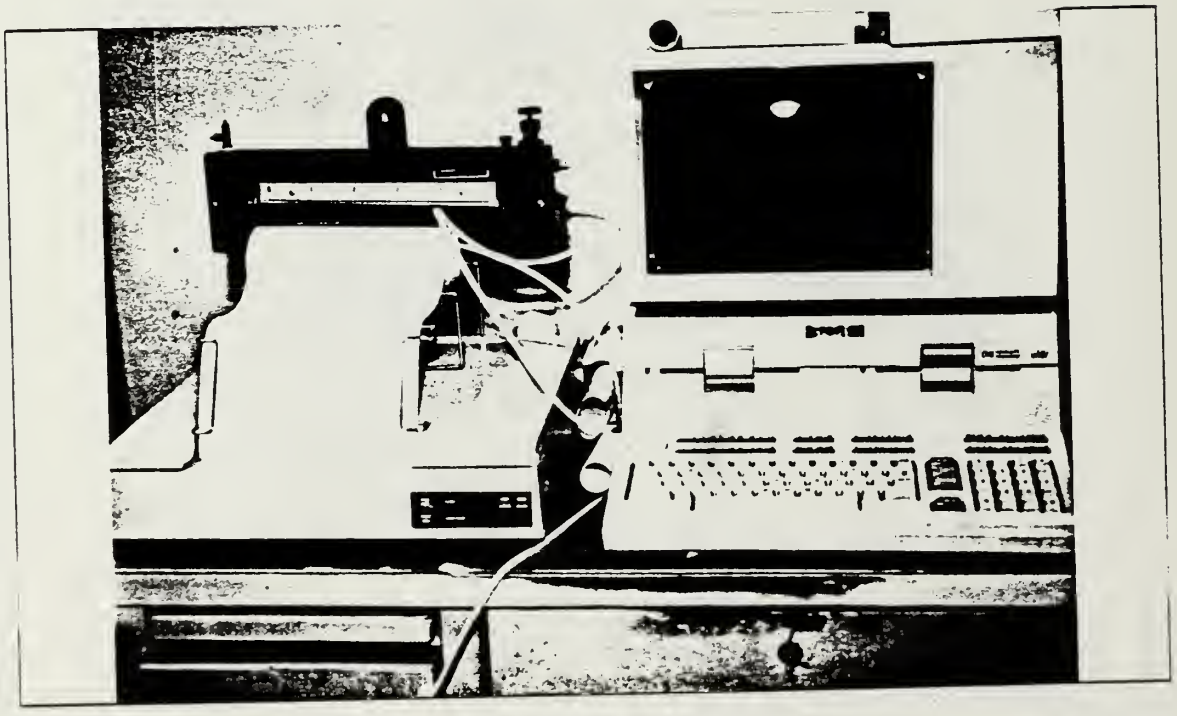

Figure 2.8 Data acquisition system.

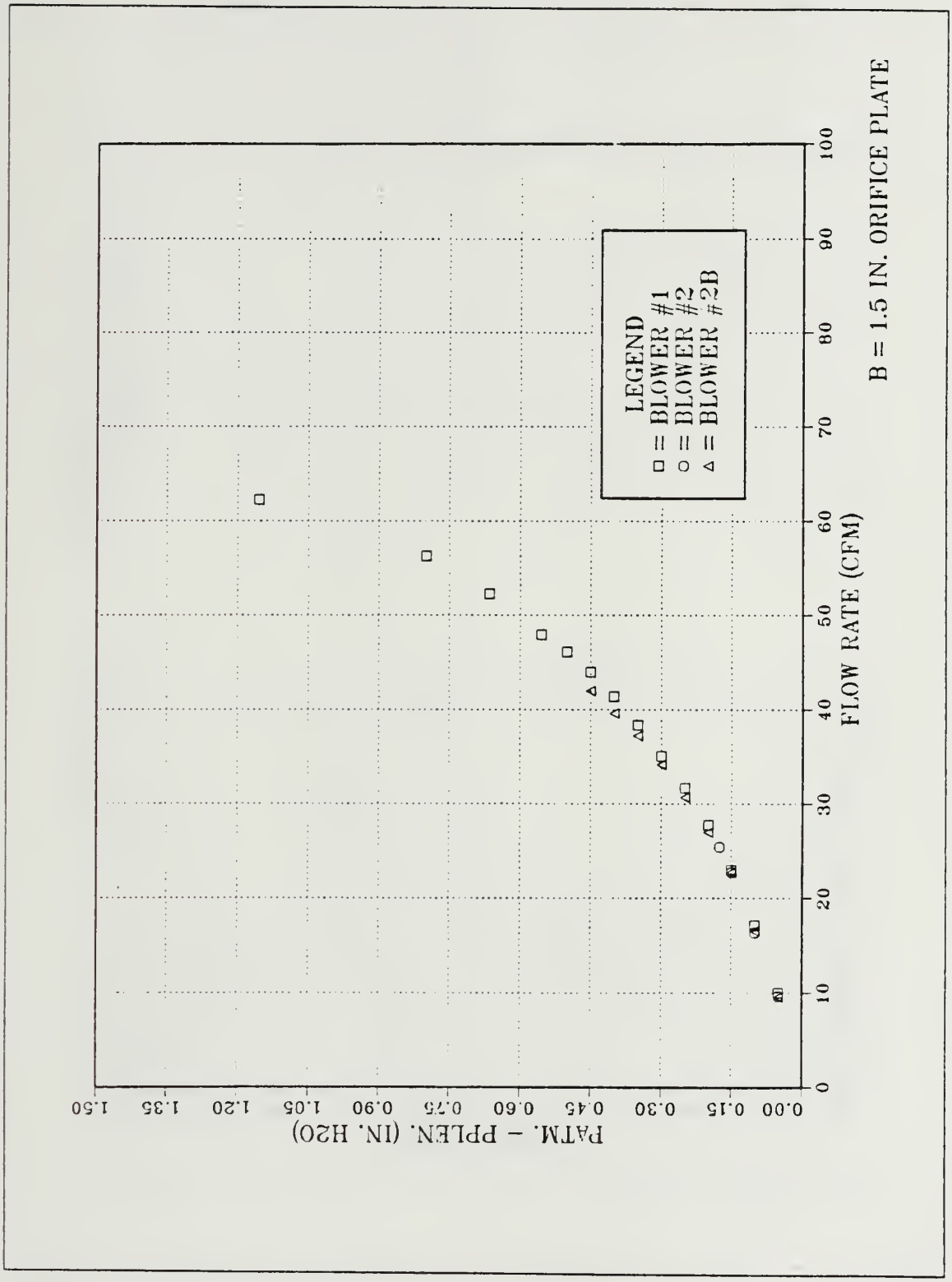

Figure 3.1 Blower comparison.

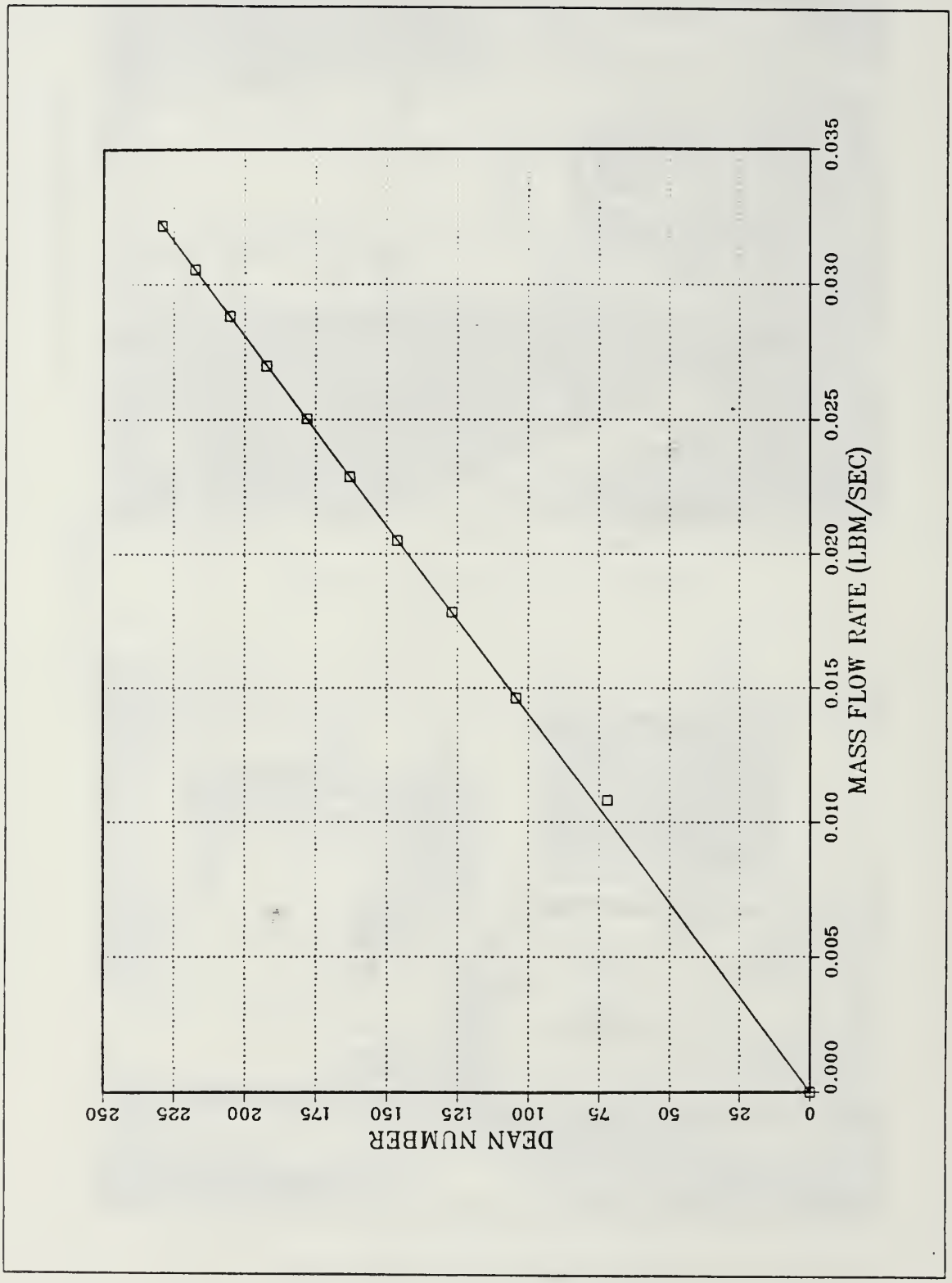

Figure 3.2 Dean number vs. channel mass flow rate.

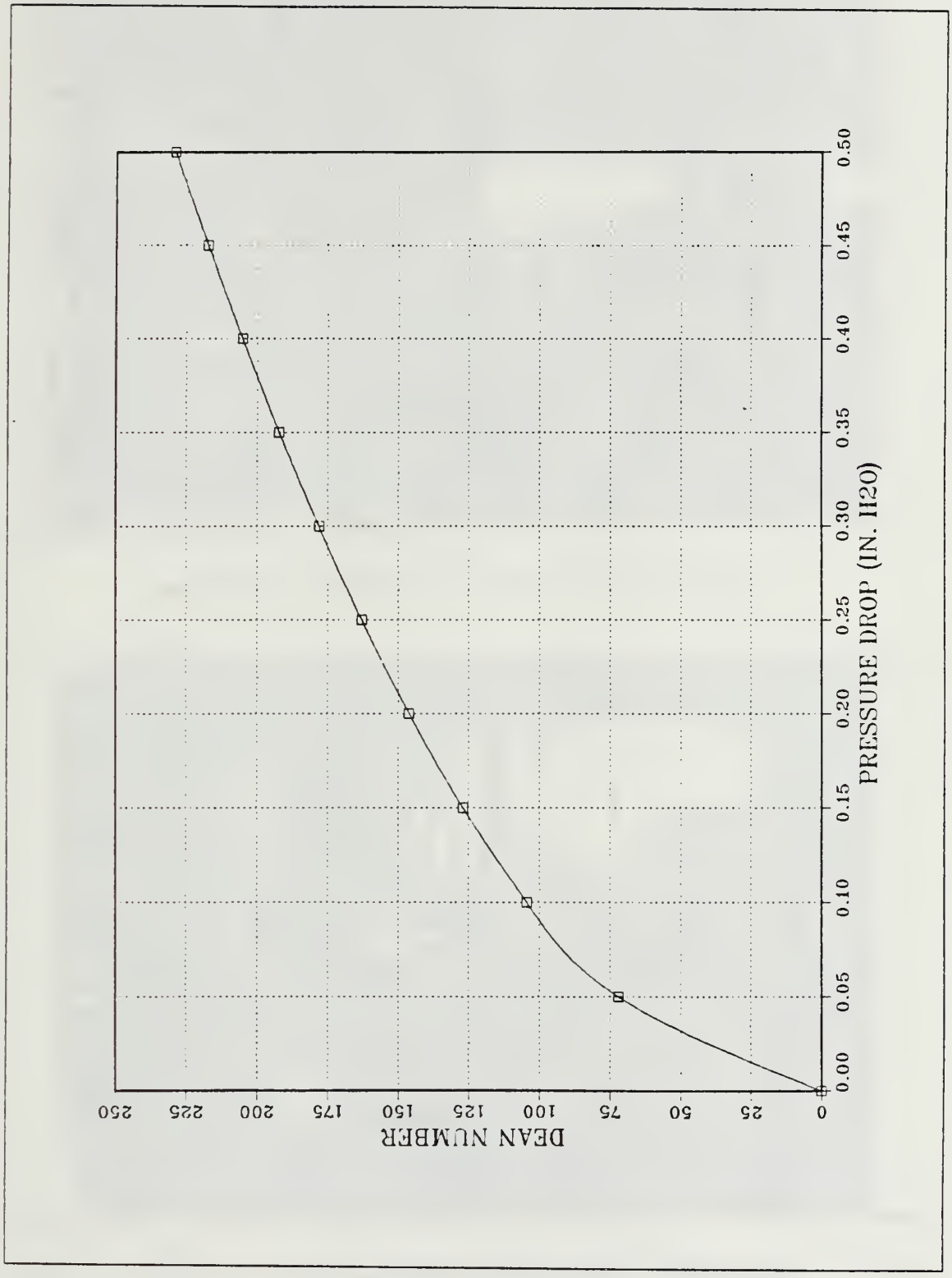

Figure 3.3 Dean number vs. orifice pressure drop.

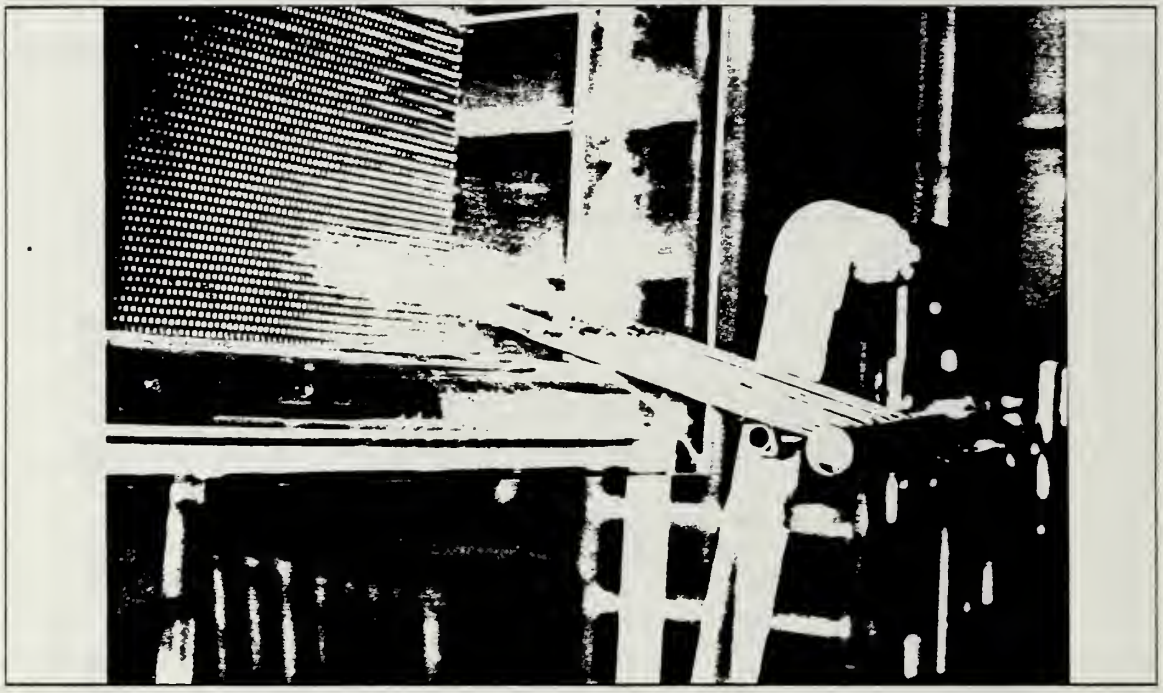

Figure 3.4 Smoke being injected into the channel mouth.

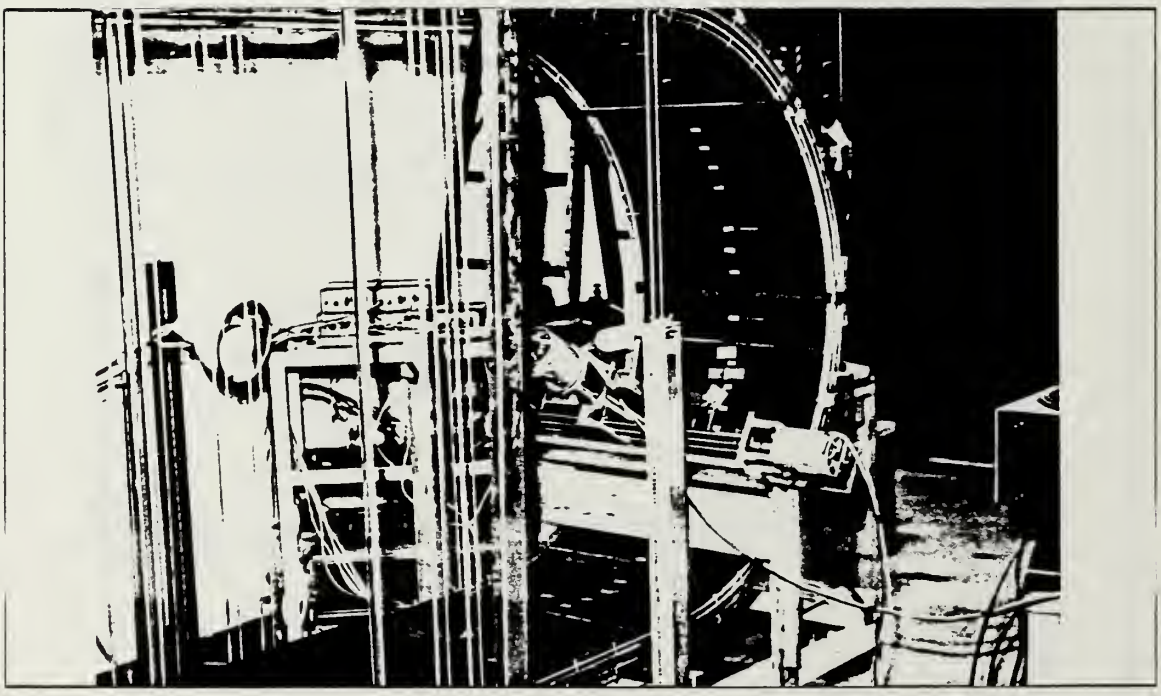

Figure 3.5 Automated traversing mechanism mounted on the channel support frame.

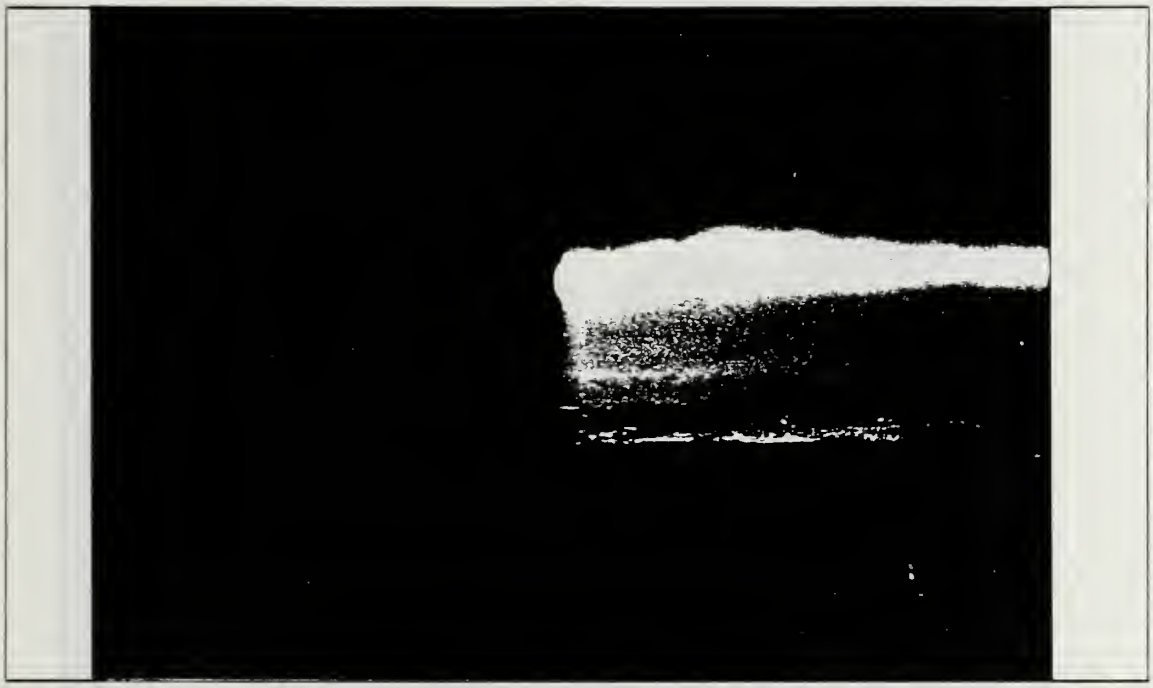

Figure 4.1 Smoke layer (Dean #42 , location 115^{o}).

Figure 4.2 Incomplete vortices (Dean #77 , location 105^{o}).

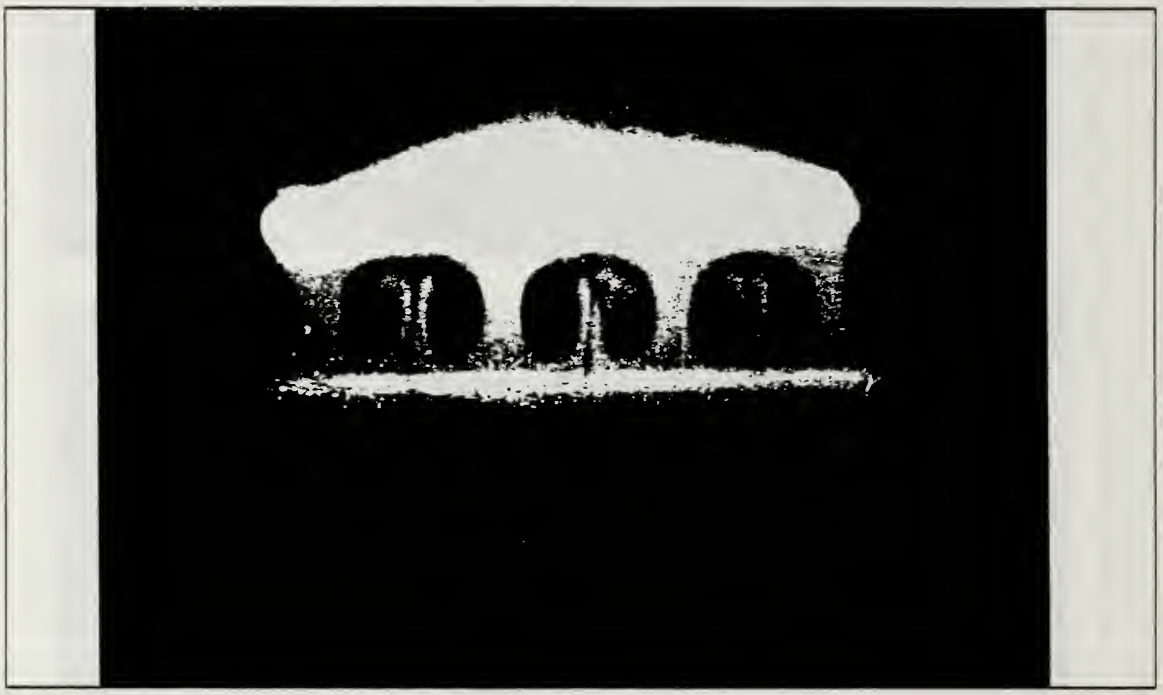

Figure 4.3 Dean vortices (Dean #73 , location 125^{o}).

Figure 4.4 Flow with turbulence (Dean #192 , location 145^{o}).

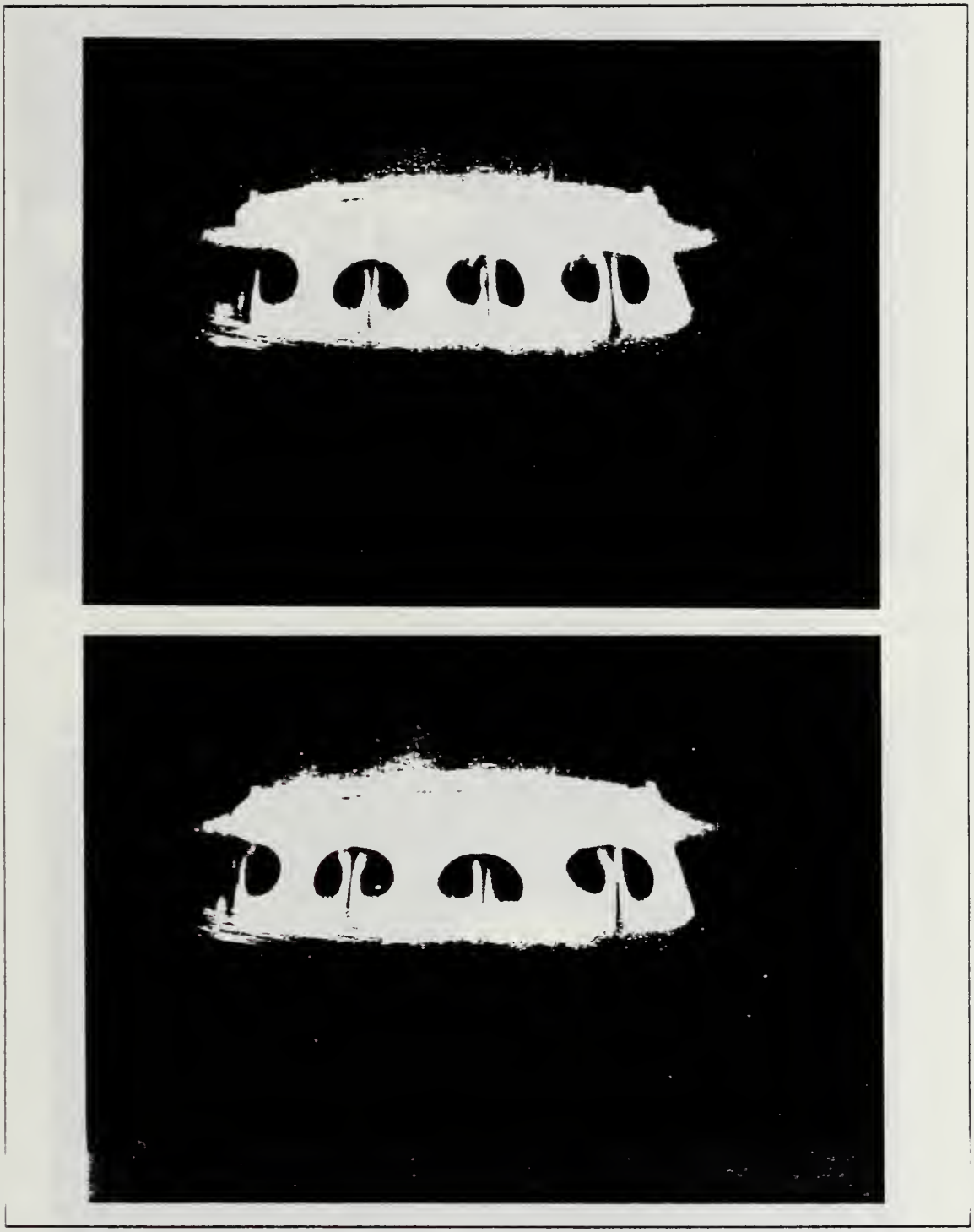

Figure 4.5 Low unsteadiness--photographs taken 3 sec. apart (Dean #122, location 95^{o}).

Figure 4.6 Moderate unsteadiness (Dean #122 , location 115^{o}).

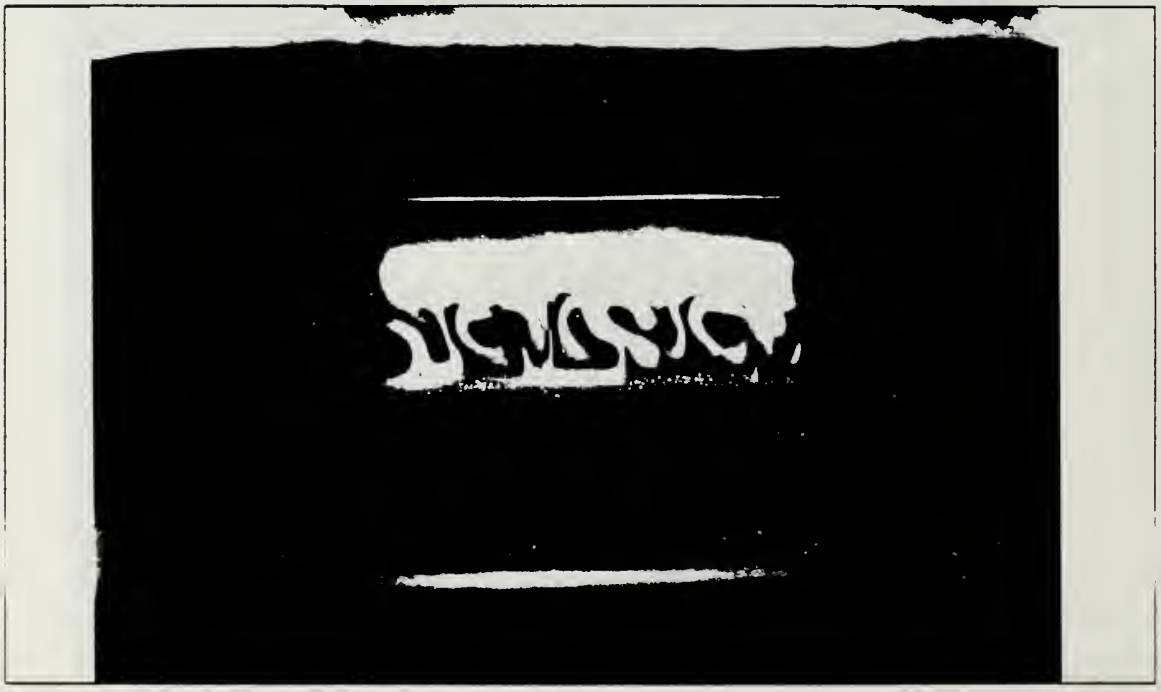

Figure 4.7 High unsteadiness (Dean #163 , location 135^{o}).

Figure 4.8 Super-High unsteadiness (Dean #163 , location 145^{o}).

Figure 4.9 Full height (Dean #123 , location 115^{o}).

Figure 4.10 Partial height (Dean #123 , location 95^{o}).

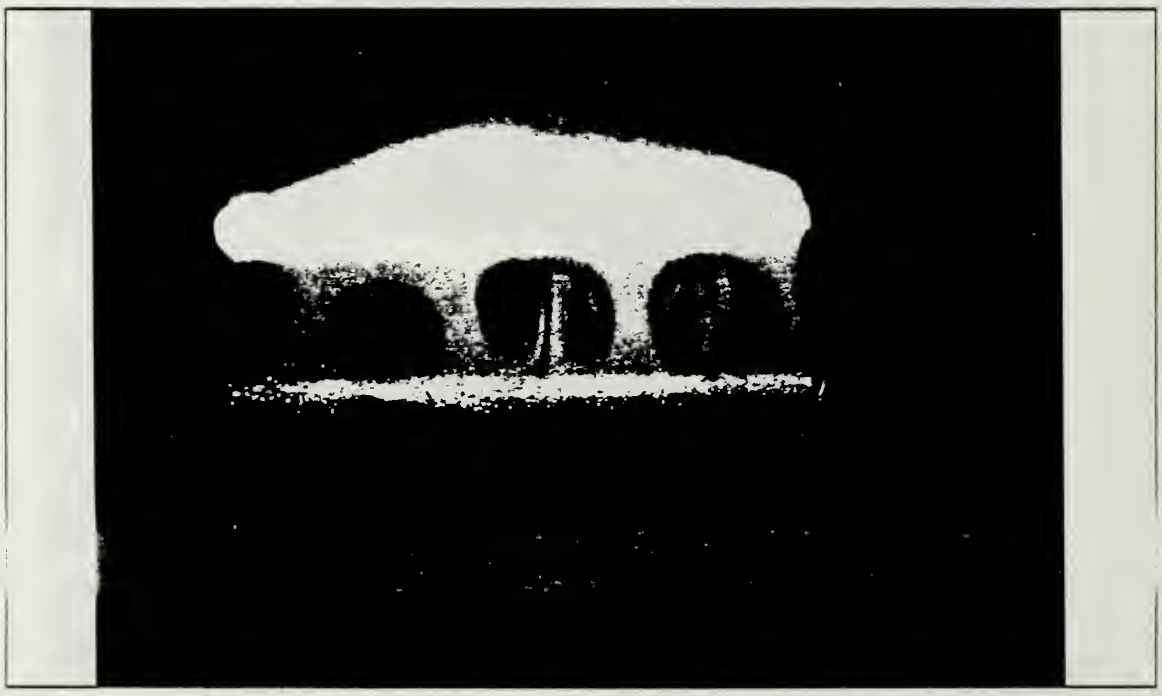

Figure 4.11 Mixed height (Dean #77 , location 125^{o}).

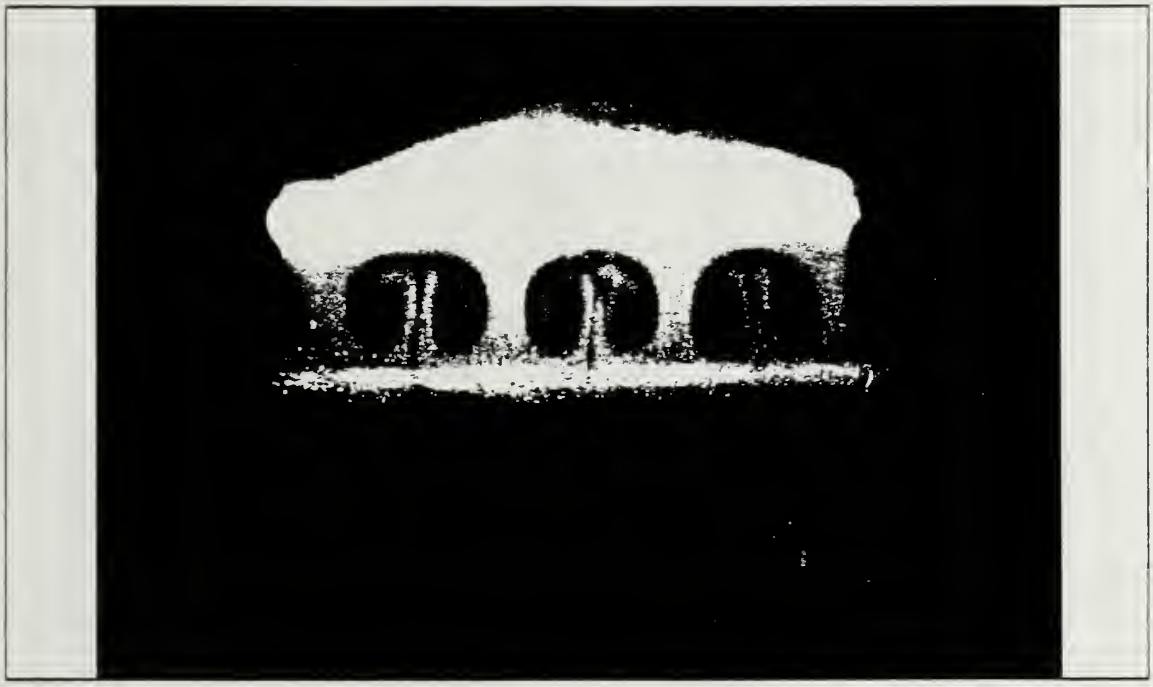

Figure 4.12 Axisymmetric vortices (Dean #77 , location 125^{o}).

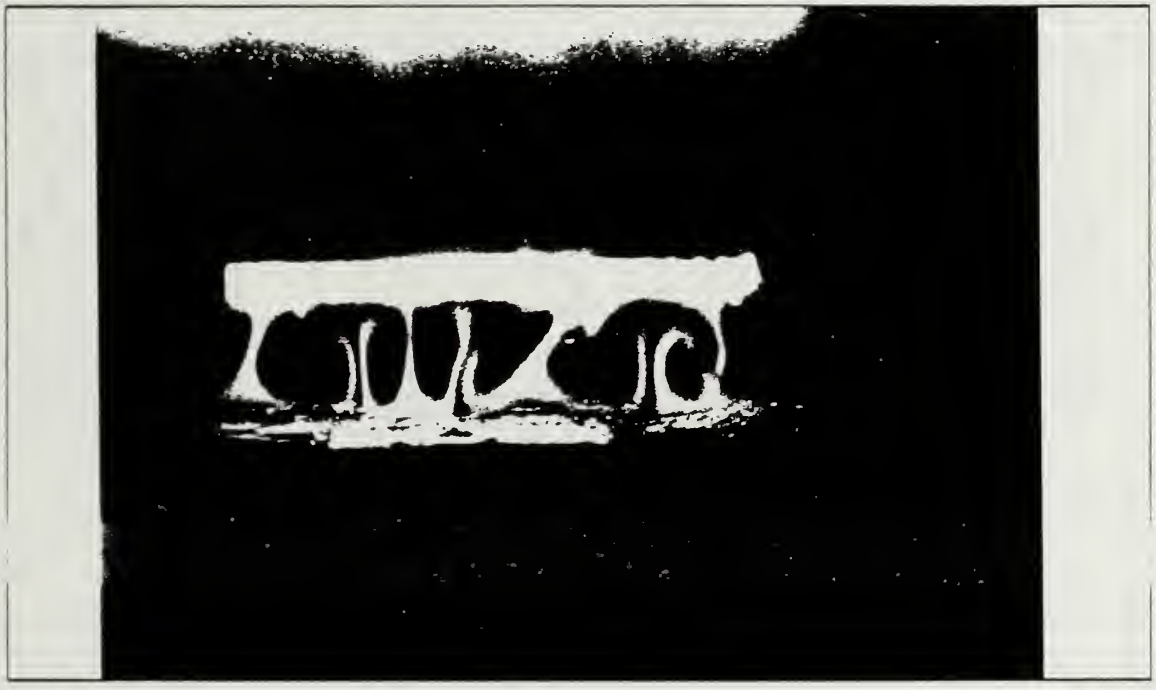

Figure 4.13 Non-Axisymmetric vortices (Dean #218 , location 105^{o}).

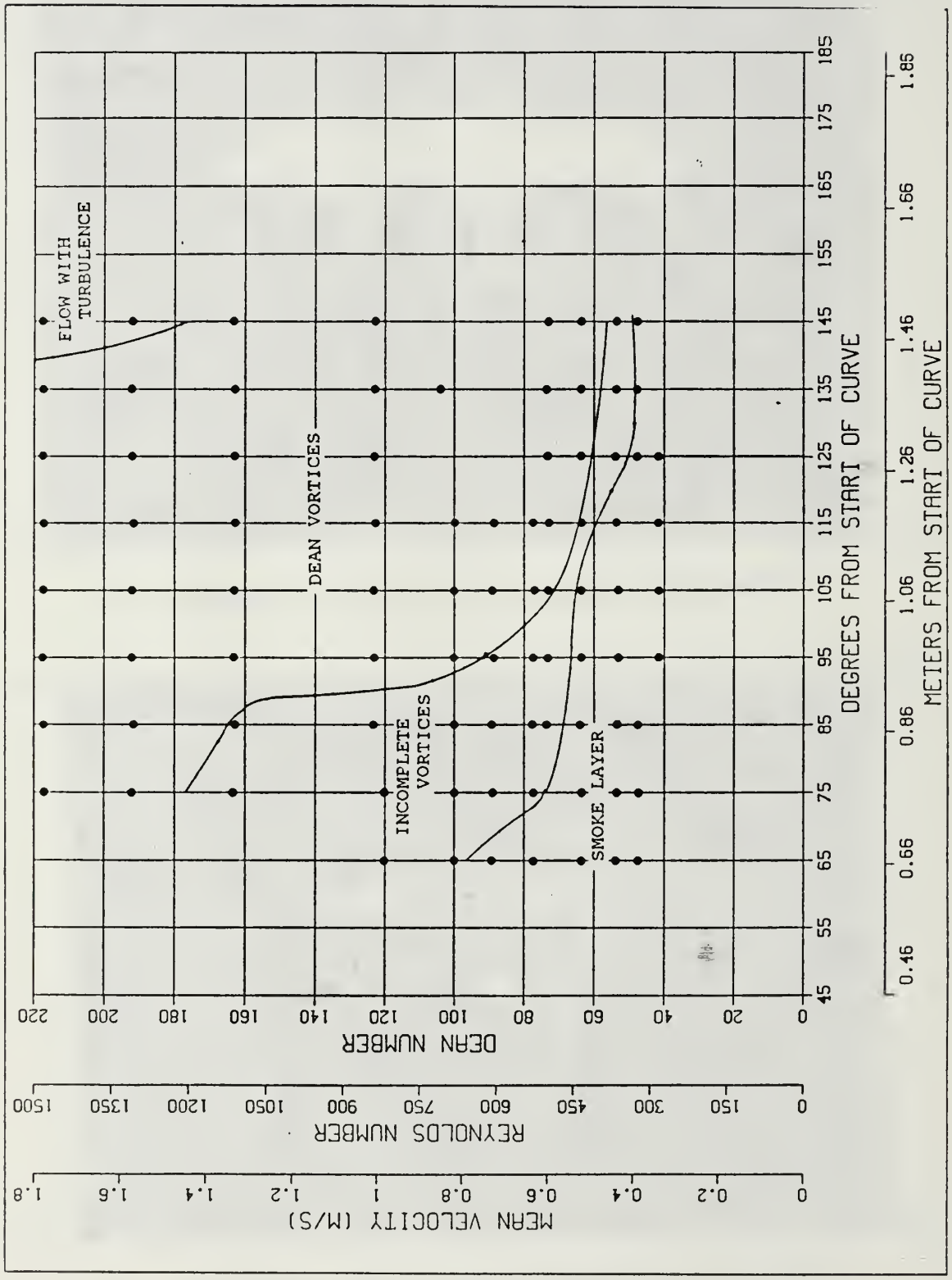

Figure 4.14 Map of the flow structure generated.

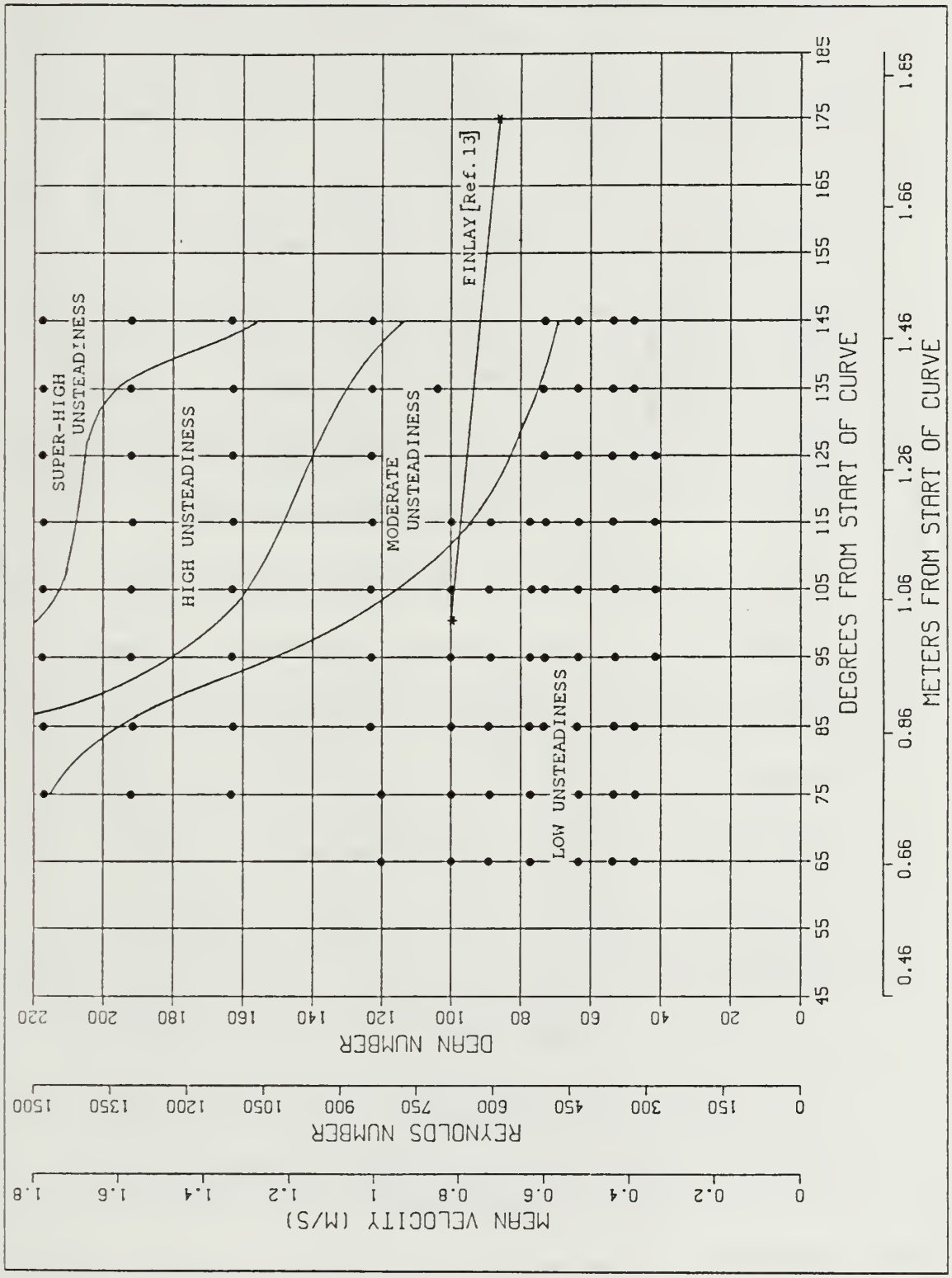

Figure 4.15 Map of the flow structure stability.

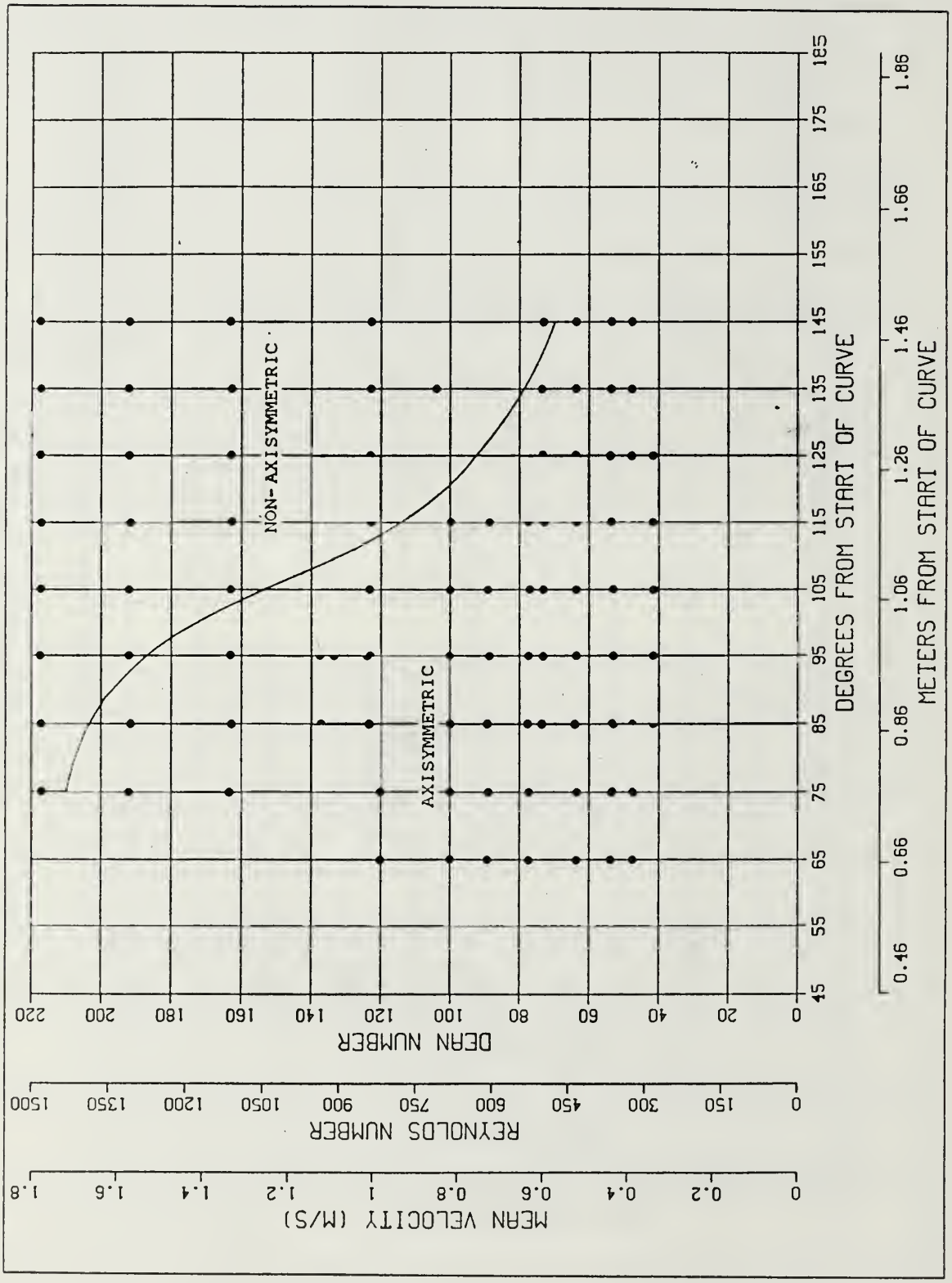

Figure 4.16 Map of the flow structure symmetry.

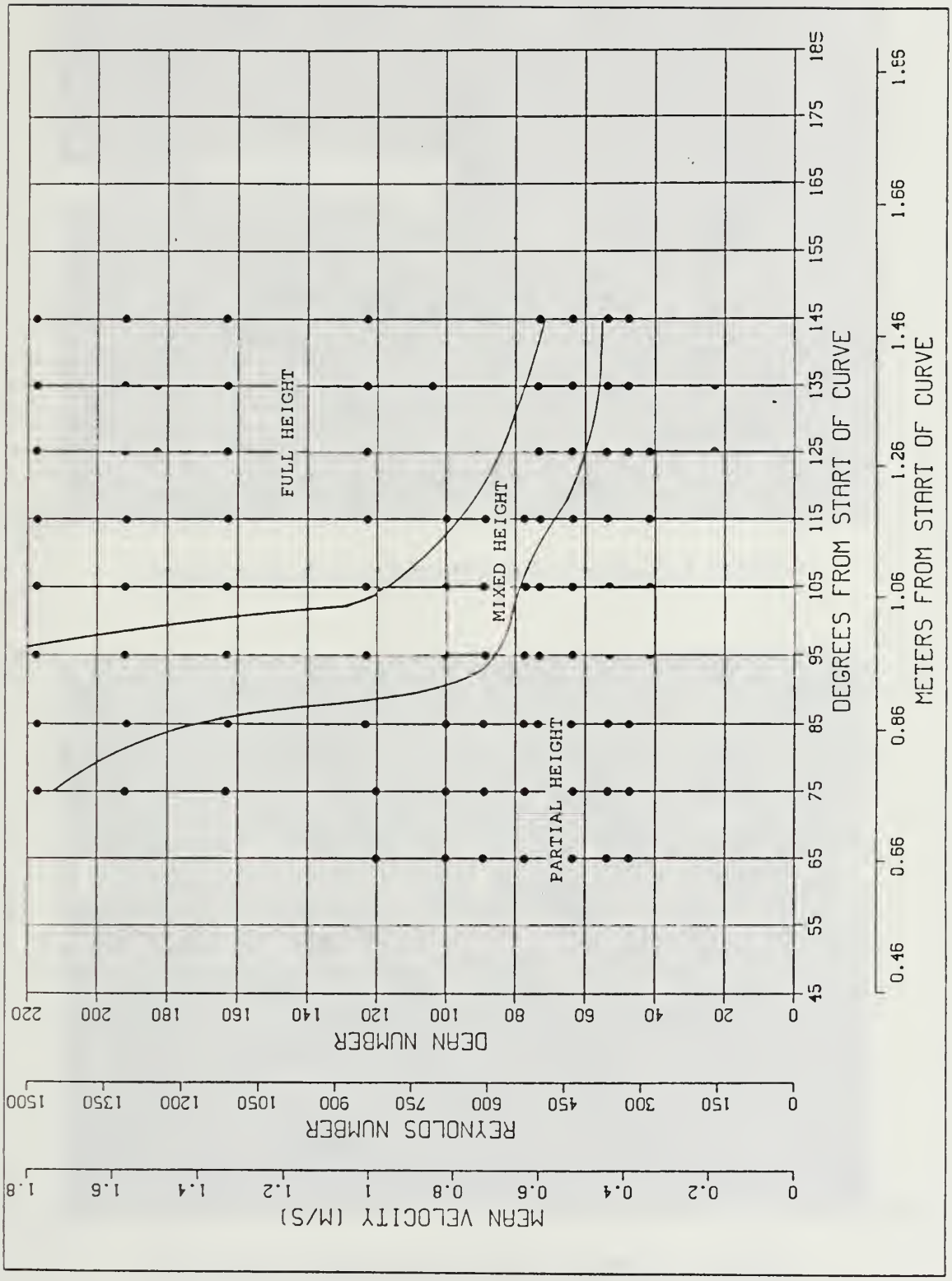

Figure 4.17 Map of the flow structure height.

Figure 4.18 Smoke flow visualization at Dean # 42 (115^{o}).

Figure 4.19 Smoke flow visualization at Dean #53 (115^{o}).

Figure 4.20 Smoke flow visualization at Dean # 64 (115^{o}).

Figure 4.21 Smoke flow visualization at Dean #73 (115^{o}).

Figure 4.22 Smoke flow visualization at Dean # 77 (115^{o}).

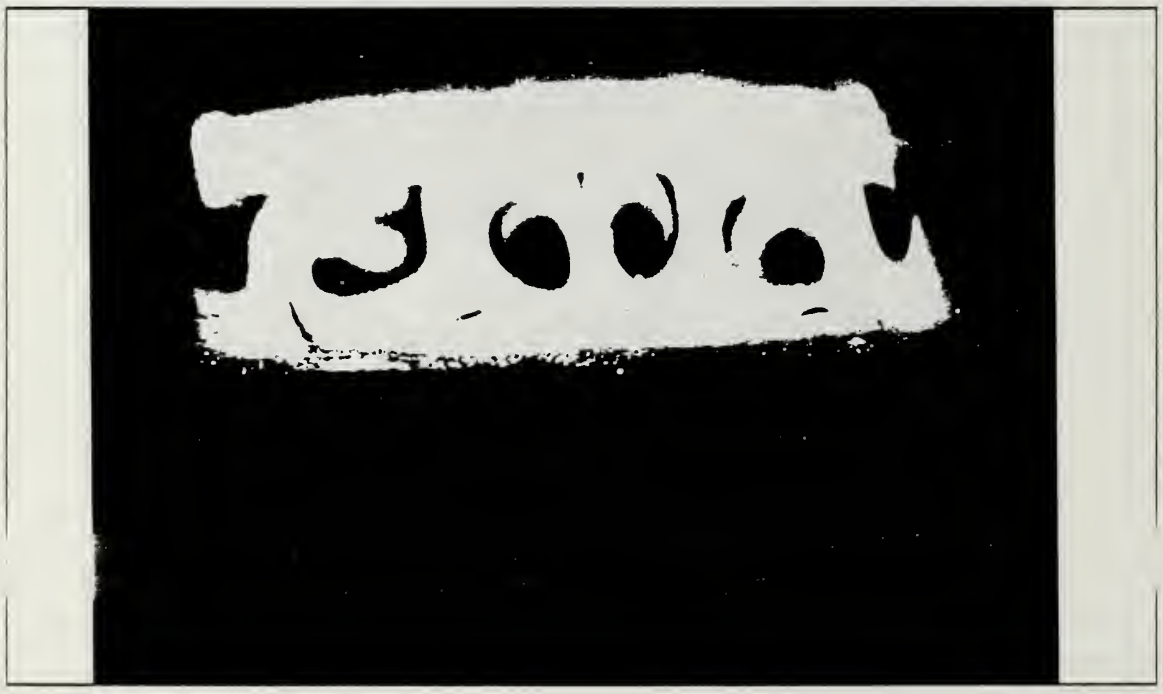

Figure 4.23 Smoke flow visualization at Dean #90 (115^{o}).

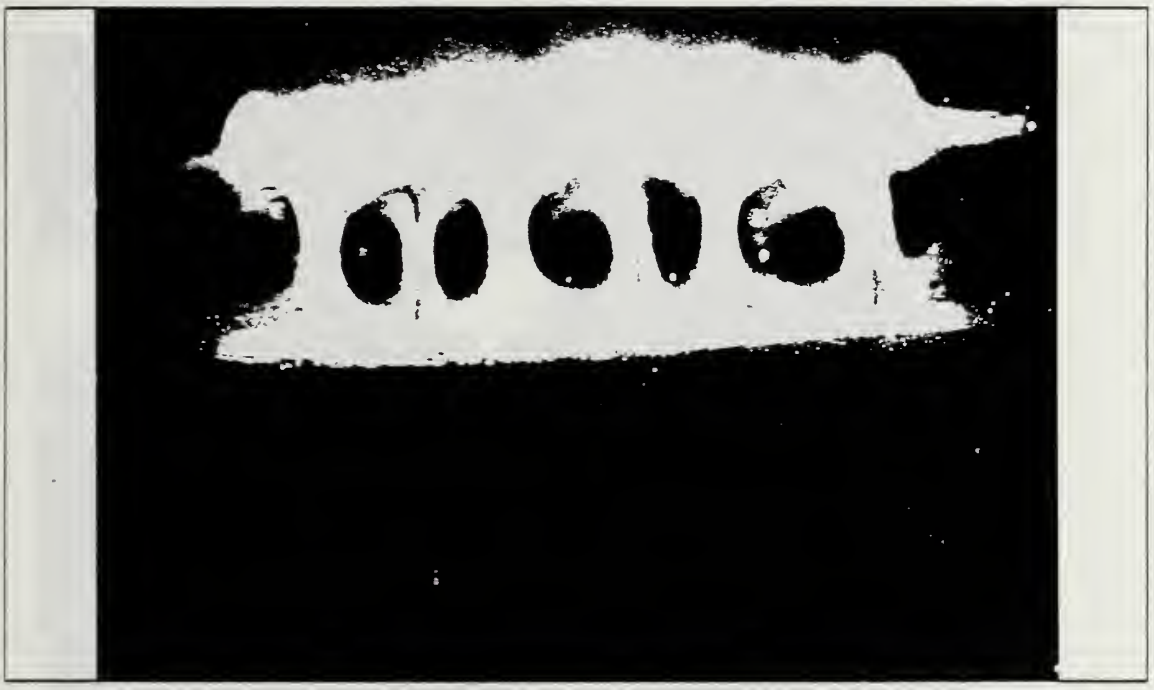

Figure 4.24 Smoke flow visualization at Dean # 100 (115°).

Figure 4.25 Smoke flow visualization at Dean #123 (115°).

Figure 4.26 Smoke flow visualization at Dean # 163 (115^{o}).

Figure 4.27 Smoke flow visualization at Dean #192 (115^{o}).

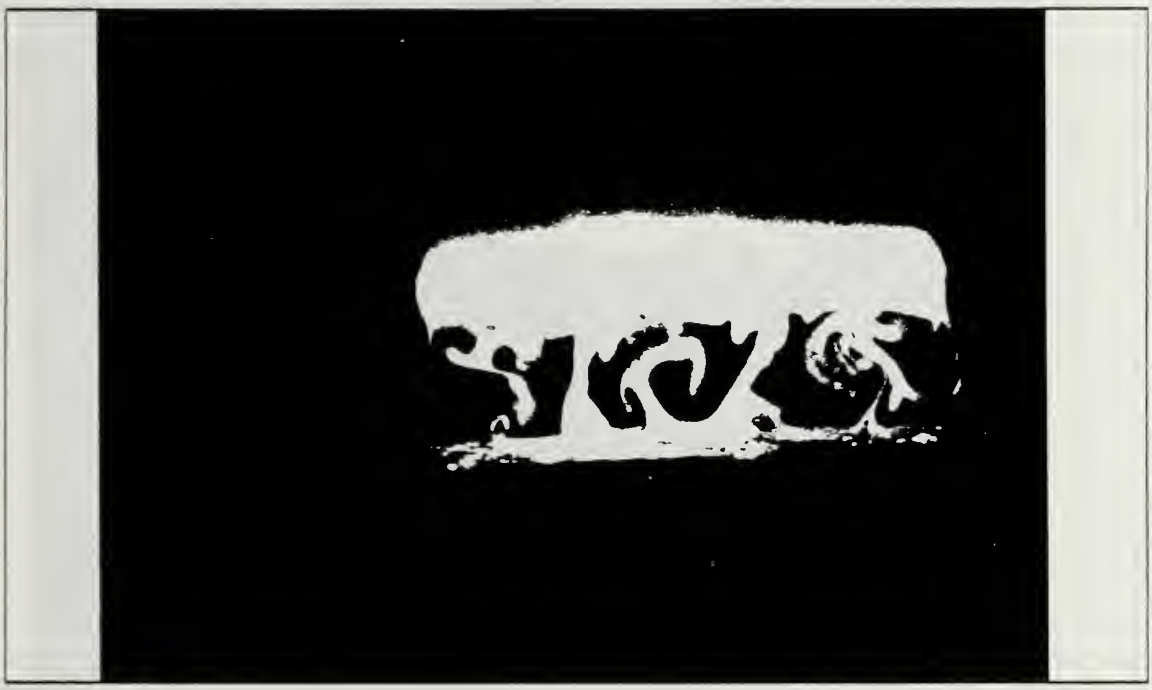

Figure 4.28 Smoke flow visualization at Dean # 218 (115^{o}).

Figure 4.29 Smoke flow visualization at 65^{o} (Dean #122).

Figure 4.30 Smoke flow visualization at 75^{o} (Dean #122).

Figure 4.31 Smoke flow visualization at 85^{o} (Dean #122).

Figure 4.32 Smoke flow visualization at 95^{o} (Dean #122).

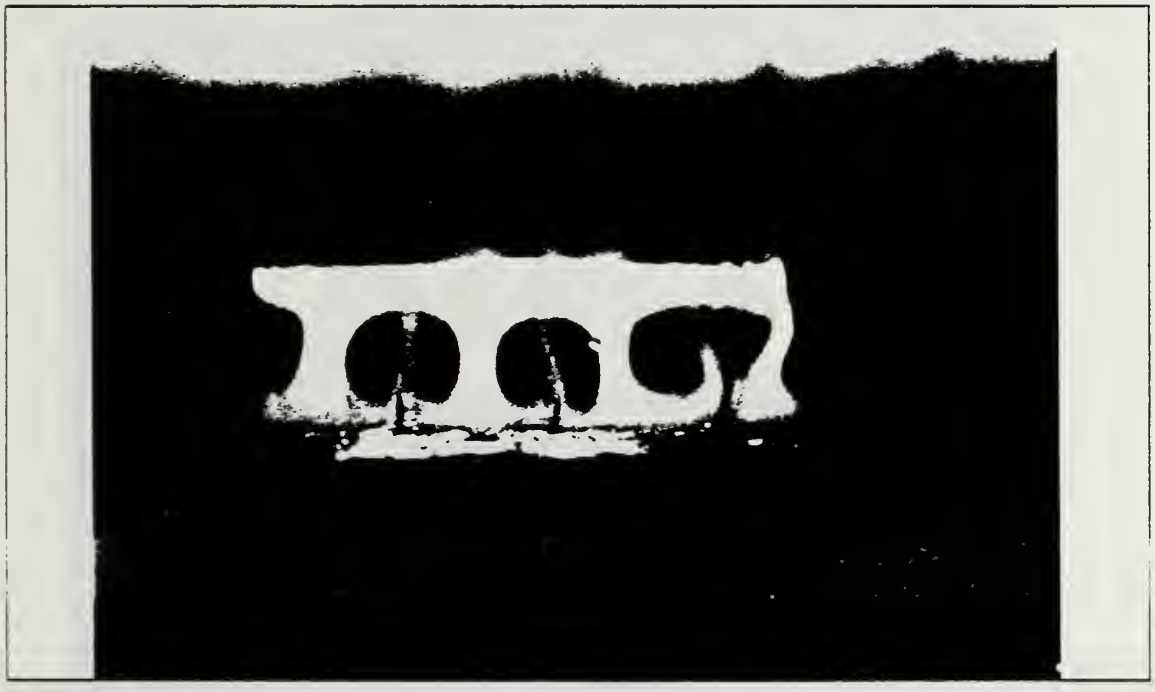

Figure 4.33 Smoke flow visualization at 105^{o} (Dean #122).

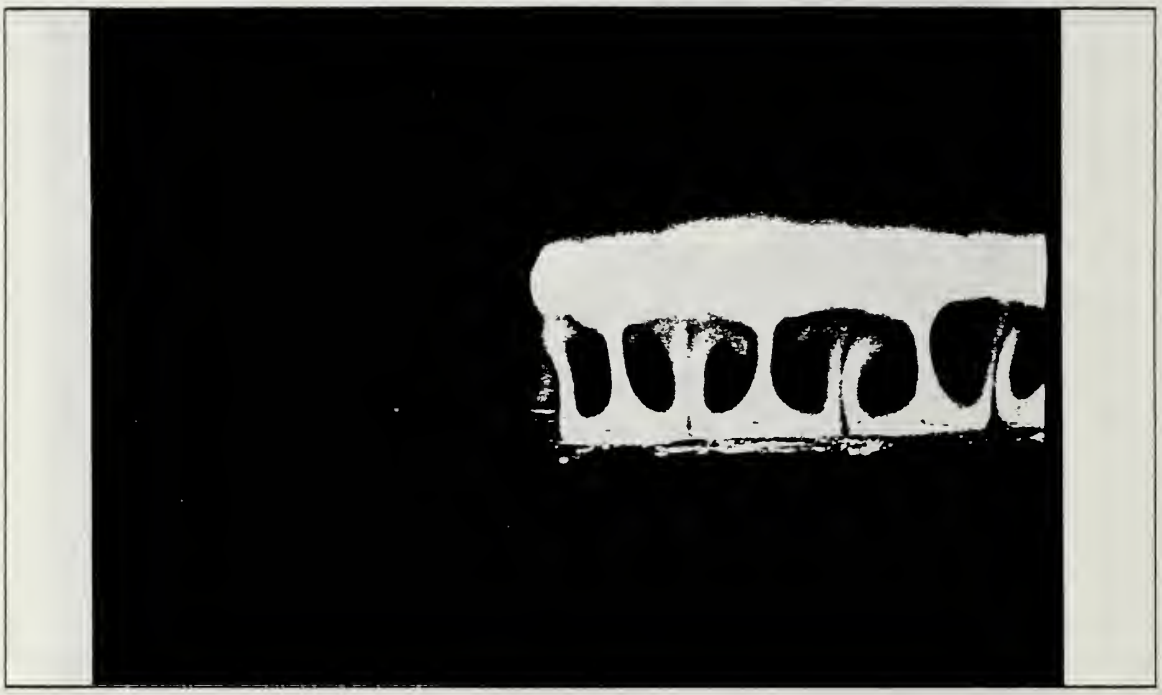

Figure 4.34 Smoke flow visualization at 115^{o} (Dean #122).

Figure 4.35 Smoke flow visualization at 125^{o} (Dean #122).

Figure 4.36 Smoke flow visualization at 135^{o} (Dean #122).

Figure 4.37 Smoke flow visualization at 145^{o} (Dean #122).

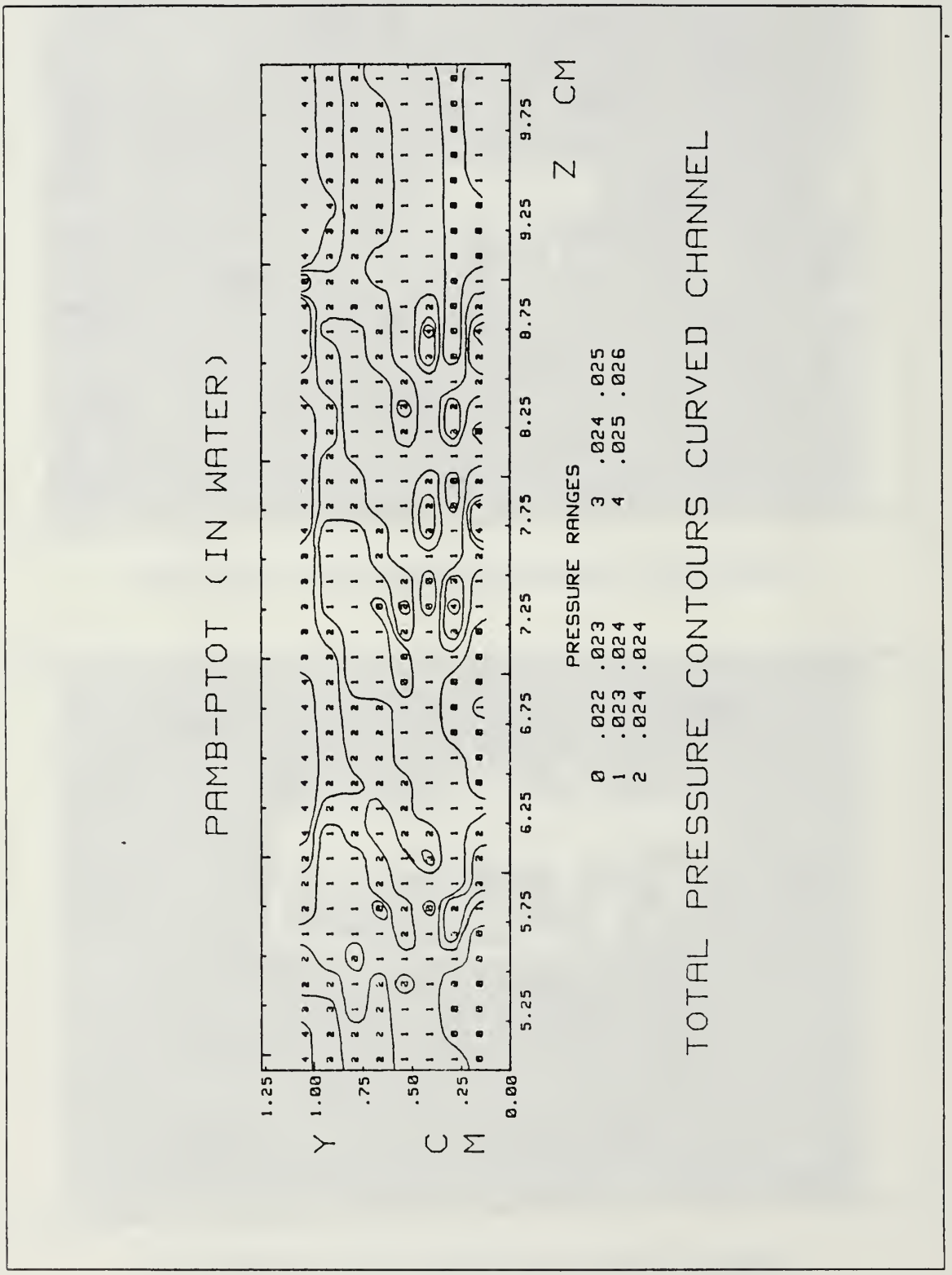

Figure 4.38 Total static pressure at the 118^{o} location.

APPENDIX B

SAMPLE CALCULATIONS FOR FLOW RATE (CFM), DEAN NUMBER, AND REYNOLD'S NUMBER (RE_C).

1. Flow Rate Calculation

$$m = A_2 K Y \sqrt{2\rho(\Delta P) g_c \, (144 \text{ in.}^2/\text{ft}^2)}$$

$A_2 = 1.227 \times 10^{-2} \, (\text{ft}^2)$

$K = .7870$ [Ref. 14]

$Y = .98$ [Ref. 15]

$\rho = .075 \, (\text{lb}_m/\text{ft}^3)$

when $P_{atm} - P_{plenum} = 0.38\text{in. } H_20$

$\Delta P = 0.05\text{in. } H_2O = 1.805 \times 10^{-3}\text{psi}$

$g_c = 32.17 \, (\text{lb}_m \, \text{ft}/\text{lb}_f \, \text{sec}^2)$

Therefore:

$m = 0.0110 \, \text{lb}_m/\text{sec} = 8.4 \text{ cfm}$

2. Reynolds number based on pipe diameter:

$$Re_D = m \, D/\rho \, A_D \, \nu$$

$m = 0.0110 \, \text{lb}_m/\text{sec}$

$D = 2.0$ in.

$A_D = 2.18 \times 10^{-2} (\text{ft}^2)$

$\nu = 1.715 \times 10^{-4} (\text{ft}^2/\text{sec})$

Therefore:

$Re_D = 6538.2$

Reynolds number based on channel height:

$$Re_{ch} = m\, d/\rho\, A_d\, \nu$$

$$A_d = 10\ in^2$$

$$d = 0.5\ in.$$

Therefore:

$$Re_{ch} = 513.1$$

4. Calculation of the Dean Number:

$$\text{Dean Number} = Re_{ch} \sqrt{d/R_i}$$

$$Re_{ch} = 513.1$$

$$d = 0.5\ in.$$

$$R_i = 23.5\ in.$$

Therefore:

Dean Number = 74.8

APPENDIX C
ACCURACY/UNCERTAINTY ANALYSIS

This section lists the uncertainty of the quantities used in flow rate, Dean number, and total pressure calculations. The quantities used in calculating flow rate and Dean number are listed in Appendix B. The uncertainties for those quantities are listed below.

$\delta A_2 = \pm 0.001\ ft^2$

$\delta K = \pm 0.001$

$\delta Y = \pm 0.02$

$\delta \rho = \pm 0.002\ lb_m/ft^2$

$\delta \Delta P = \pm 1.0\ lb_m/ft^2$

Therefore

$\delta m = \pm 0.0005\ lb_m/sec$ (95% confidence level)

$\delta Dean\ \# = \pm 5\%$ (95% confidence level)

Total pressure was calculated using the following equation. The uncertainties for each quantity are also listed.

$Press = C(V-V_o)$

$\delta C = \pm 0.02$ in. H_2O/Volt

$\delta V = \pm 0.002$ Volts

$\delta V_o = \pm 0.001$ Volt

$\delta P_{drift} = \pm 0.0005$ in. H_2O

Therefore

$\delta P = \pm 0.0005$ in. H_2O (95% confidence level)

LIST OF REFERENCES

1. Holihan, R.G., Jr., *Investigations of Heat Transfer in Straight and Curved Rectangular Ducts for Laminar and Transition Flows*, Master's Thesis, Naval Postgraduate School, Montery, California, 1981.

2. Dean W.R., "Fluid Motion in a Curved Channel," *Proceedings of the Royal Society of London*, Series A, V. 121, pp. 402-420, 1928.

3. Finlay, W.H., Keller, J.B., and Ferziger, J.H., *Finite Amplitude Vortices in Curved Channel Flow*, Department of Mechanical Engineering, Stanford University, Stanford, California, 1986.

4. Kelleher, M.D., Flentie, D.L., and Mckee, R.J., "An Experimental Study of the Secondary Flow in a Curved Rectangular Channel," *Journal of Fluid Engineering*, V. 101, pp. 92-96, March 1980.

5. Nakabayashi, K., "Transition of Taylor-Gortler Vortex Flow in Spherical Couette Flow," *Journal of Fluid Mechanics*, V. 132, pp. 209-230, 1983.

6. Williams, D.R., Fasel H., and Hama F.R., "Experimental Determination of the Three-Dimensional Vorticity Field in the Boundary-Layer Transition Process," *Journal of Fluid Mechanics*, V. 149, pp. 179-203, 1984.

7. Nishioka, M., and Asai, M., "Some Observations of the Subcritical Transition in Plane Poiseuille Flow," *Journal of Fluid Mechanics*, V. 150, pp. 441-450, 1985.

8. Hille, P., Vehrenkamp, R., and Schulz-Dubois, E.O., "The Development and Structure of Primary and Secondary Flow in a Curved Square Duct," *Journal of Fluid Mechanics*, V. 151, pp. 219-241, 1985.

9. Georgiou, G.A., and Eagles, P.M., "The Stability of Flows in Channels with Small Wall Curvature," *Journal of Fluid Mechanics*, V. 159, pp. 259-287, 1985.

10. Siedband, M.A., *A Flow Visualization study of Laminar/Turbulent Transition in a Curved Channel*, Master's Thesis, Naval Postgraduate School, Monterey, California, March 1987.

11. Morrison, G. A., *On The Use of Liquid Crystal Thermography as A Technique of Flow Visualization*, Master's Thesis, Naval Postgraduate School, Monterey, California, June 1984.

12. Evens, D.L., *Study of Vortices Embedded in Boundary Layers With Film Cooling*, Master's Thesis, Naval Postgraduate School, Monterey, California, March 1987.

13. Finlay, W.H., private communication, Department of Mechanical Engineering, Stanford University, Stanford, California, 1987.

14. ASME Power Test Codes Committee, ASME Power Test Codes, (*Supplement on Instruments and Apparatus*), part 5, Chapter 4, p. 25, American Society of Mechanical Engineers, 1959.

15. Holman, J.P., and Gajda, W.J., Jr., *Experimental Methods for Engineers*, 4th Edition, pp. 238-247, McGraw Hill, 1984.

INITIAL DISTRIBUTION LIST

		No. Copies
1.	Defense Technical Information Center Cameron Station Alexandria, VA 22304-6145	2
2.	Library, Code 0142 Naval Postgraduate School Monterey, CA 93943-5002	2
3.	Professor P.M. Ligrani Code 69SLi Department of Mechanical Engineering Naval Postgraduate School Monterey, CA 93943-5000	8
4.	Department Chairman Code 69 Department of Mechanical Engineering Naval Postgraduate School Monterey, CA 93943-5000	1
5.	Dr. K. Civinskas Propulsion Directorate U.S. Army Aviation Res & Technology Activity AVSCOM NASA-Lewis Research Center Cleveland, OH 45433	10
6.	Lt. Randal D. Niver, USN 4010 N. 21st Drive Phoenix, AZ 85015	4

Thesis
N5975 Niver
c.1 Structural characteristics of dean vortices in a curved channel.